Novel tetranuclear copper |2+4| cubanes resulting from unprecedented C-O bond formation *cum* dearomatization

Amit Kumar, Rampal Pandey, Rakesh Kumar Gupta, Mrigendra Dubey, and Daya Shankar Pandey*

Department of Chemistry, Faculty of Science, Banaras Hindu University, Varanasi - 221 005, India

Supporting Information Placeholder

Contents:

Experimental Section

General methods and materials

Common reagents and solvents were acquired from commercial sources and solvents were dried and distilled using literature procedures.[1] Elemental analyses for C, H and N were on a CE-440 Elemental Analyzer. Infrared and electronic absorption spectra were obtained on a Perkin-Elmer Spectrum Version 10.03.05 FT-IR and Shimadzu UV-1601 spectrophotometer, respectively. The ^{1}H (300 MHz) and ^{13}C (75.45 MHz) NMR spectra were obtained on a JEOL AL300 FT-NMR spectrometer using tetramethylsilane (TMS) as an internal reference. The fluorescence spectra were obtained on a PerkinElmer LS 55 Fluorescence Spectrometer (U.K.). Electrospray ionization mass spectrometric data were obtained on a JEOL Accu TOF JMS-T100 LC mass spectrometer. Electrochemical measurements were made on CHI 620c electrochemical analyzer using single compartment cell equipped with a glassy carbon working, platinum wire counter, and Ag/Ag^{+} reference electrode under nitrogen atmosphere. Electrical conductivity (solution) was measured on a Eutech Instruments CON 5/TDS 5 conductivity meter in methanol.

Preparation of 4-(3-Amino-2,4,6-trimethylphenylimino)-pent-2-en-2-ol (H_3L1)

To a methanolic solution (20 mL) of 2,4,6-trimethylbenzene-1,3-diamine (0.751 g, 5.0 mmol), acetylacetone (0.51 mL, 5.0 mmol) and catalytic amounts of acetic acid were added and the contents of the flask heated under reflux for 6h. After cooling to rt it gave white block shaped crystals which were separated, washed by diethyl ether and dried under vacuo. Yield (1.044 g; 90%). Anal. Calcd. [$C_{14}H_{20}N_2O$]: C 72.38, H 8.68, N 12.06%; Found: C 72.22, H 8.58, N 11.98%.^{1}H NMR ($CDCl_3$, δH ppm): 11.90 (s, 1H, O*H*), 6.82 (s, 1H) 5.18 (s, 1H), 3.53 (s, 2H, NH_2), 2.16 (s, 3H), 2.10 (s, 3H), 2.08 (s, 6H), 2.03 (s, 3H). ^{13}C NMR ($CDCl_3$, δC ppm): 195.7, 163.4, 141.2, 134.5, 129.3, 124.8, 121.1, 119.6, 95.3, 28.9, 18.9, 17.5, 17.5, 12.4. ESI-MS (Calcd., Found, *m/z*): 233.1609, 233.1657 [$(M+H)^{+}$, 100%]. IR (KBr pellets, cm^{-1}): 3454 (s), 3351 (s), 1736 (w), 1606 (s), 1538 (s), 1481(s), 1273 (m), 1116 (s), 868 (m), UV/vis. (MeCN, λ_{max}, nm, ε $M^{-1}cm^{-1}$): 307 (5.09×10^3).

Preparation of 4-[3-(3-hydroxy-1-methyl-but-2-enylideneamino)-2,4,6-trimethylphenyl-imino] -pent-2-en-2-ol (H_2L2)

It was prepared following the above procedure for **H_3L1** except that diamine and acetyl acetone were taken in 1:2 molar ratio and contents of the flask were heated under reflux for 24 h. After cooling to rt it gave a red oily product. The desired compound was obtained from the oily product by extraction and purification using hexane. Yield (1.256 g; 80%). Anal. Calcd. [$C_{19}H_{26}N_2O_2$]: C 72.58, H 8.33, N 8.91%; Found: C 72.49, H 8.29, N 8.84%. ^{1}H NMR ($CDCl_3$, δH ppm): 11.89 (s, 2H), 6.99 (s, 1H,) 5.22 (s, 1H), 2.17 (s, 3H), 2.11(s, 3H), 2.04 (s, 3H), 1.61 (s, 6H). ^{13}C NMR ($CDCl_3$, δC ppm): 195.7, 162.3, 141.0, 135.1, 134.6, 129.4, 95.7, 37.2, 18.5, 17.7, 17.5, 13.8. ESI-MS (Calcd., Found, m/z): 315.2028, 315.2076 [$(M+H)^+$, 76%]. IR (KBr pellets, cm^{-1}): 3455, 3151, 2957, 1610, 1561, 1481, 1273, 1118, 1014, 871. UV/vis. (MeCN, λ_{max}, nm, ε $M^{-1}cm^{-1}$): 309 (6.25×10^3).

Preparation of 4-{3-[(4-{[3-(3-Hydroxy-1-methyl-but-2-enylideneamino)-2,4,6-tri-methylphenylimino]-methyl}-benzylidene)-amino]-2,4,6-trimethylphenylimino}-pent-2-en-2-ol (H_2L3)

A methanolic (10 mL) solution of teraphthaldehyde (0.268 g, 2.0 mmol) was added into the solution of **H_3L1** (0.928 g, 4.0 mmol) in methanol (10 mL) with catalytic amounts of acetic acid and the contents of the flask was heated under reflux for 12 h. After cooling to rt it gave a yellow oily product. The desired compound was obtained from the oily product by extraction and purification using hexane. Yield (0.922 g; 82%). Anal. Calcd. [$C_{36}H_{42}N_4O_2$]: C 76.84, H 7.52, N 9.96%; Found: C 76.78, H 7.44, N 9.87%. ^{1}H NMR ($CDCl_3$, δH ppm): 11.90 (s, 2H), 8.25 (s, 2H), 8.04 (s, 4H), 6.98 (s, 2H), 5.21 (s, 2H), 2.16 (s, 6H), 2.11 (s, 6H), 2.08 (s, 6H), 2.03 (s, 6H), 1.67(6H). ^{13}C NMR ($CDCl_3$, δC ppm): 195.9, 162.4, 149.4, 138.3, 134.6, 131.1, 129.6, 125.3, 124.7, 121.0, 95.6, 28.9, 18.8, 18.0, 17.5, 13.5. ESI-MS (Calcd., Found, m/z): 563.3341, 563.3387 [$(M+H)^+$, 42%]. IR (KBr pellets, cm^{-1}): 3352 (w), 2920 (w), 1607 (s), 1557 (s), 1480 (m), 1298 (s), 1274 (s), 1091 (m), 736 (m): UV/vis. (MeCN, λ_{max}, nm, ε $M^{-1}cm^{-1}$): 303 (4.20×10^3)

Preparation of $[Cu(H_2L1O)]_4 \cdot 4NO_3 \cdot 2H_2O$ (1).

Following general procedure was used for the preparation of **1**.

To a deprotonated stirring solution of the ligands **H_3L1**, **H_2L2** and **H_2L3** [prepared by treatment of the respective ligands (**H_3L1**, 0.232 g, 1.0 mmol; **H_2L2**, 0.157 g, 0.5 mmol; or **H_2L3**, 0.281 g, 0.5 mmol) with KOH (0.056 g, 1.0 mmol) in methanol (10 mL) under stirring

over half an hour] a methanolic solution (10 mL) of $Cu(NO_3)_2.2.5H_2O$ (0.232 g, 1.0 mmol) was added dropwise and stirred at rt additionally for 1h. Slowly, the reaction mixture turned dark brown. It was filtered it to remove any solid impurities and the filterate concentrated to ~10 mL and left undisturbed for crystallization. After two days black block shaped crystals appeared which were separated, washed with diethyl ether and dried under vacuo.

Note: Irrespective of the deprotonated lignads **H_3L1**, **H_2L2** and **H_2L3**, their reaction with $Cu(NO_3)_2 \cdot 2.5H_2O$ under analogous conditions gave the same product **1** in an appreciable yield (based on the starting ligand) [**H_3L1**, 0.289 g, 85%; **H_2L2**, 0.259 g, 76%; **H_2L3**, 0.231 g, 68%). Anal. Calcd. [$C_{56}H_{80}Cu_4N_{12}O_{22}$]: C 44.03, H 5.28, N 11.00, Found: C 44.14, H 5.32, N 11.07%. ESI-MS (Calcd, Found, *m/z*): 1239.2973, 1239.2887 [$(M–3H)^+$, 35%]; IR (KBr pellets, cm^{-1}): 3416 (br), 1646 (w), 1576 (m), 1522 (m), 1384 (s), 1083 (w), 1035 (w). UV/vis. (MeCN, λ_{max}, nm, ε $M^{-1}cm^{-1}$): 430 (4.07×10^3), 352 (4.52×10^3), 279 (9.20×10^3). Λ_M (MeOH, $ohm^{-1}cm^2mol^{-1}$): 411.

Preparation of $[Cu(HL1O)]_4 \cdot 4H_2O$ (2)

It was prepared following the above procedure for **1** using deprotonated **H_3L1**, **H_2L2** and **H_2L3** [prepared by treatment of the respective ligands (**H_3L1**, 0.232 g, 1.0 mmol; **H_2L2**, 0.157 g, 0.5 mmol; or **H_2L3**, 0.281 g, 0.5 mmol) with KOH (0.56 g, 1.0 mmol) in methanol (10 mL) under stirring over half an hour] and methanolic solution (10 mL) of $Cu(acac)_2 \cdot H_2O$ (0.262 g, 1.0 mmol) in place of $Cu(NO_3)_2 \cdot 2.5H_2O$ (0.232 g, 1.0 mmol) and stirring the reaction mixture for 8h. In this case also, we ended up with the same product **2**. Yield based on the starting ligand (**H_3L1**, 0.269 g, 87%; **H_2L2**, 0.232 g, 75%; **H_2L3**, 0.217 g, 70%). Anal. Calcd. [$C_{56}H_{80}Cu_4N_8O_{12}$]: C 51.29, H 6.15, N 8.54%, Found: C 51.37, H 6.19, N 8.59%. ESI-MS (Calcd., Found, *m/z*): 1239.2973, 1239.2827 [$(M+H)^+$, 31%]. IR (KBr pellets, cm^{-1}): 3434 (br), 1626 (w), 1571 (s), 1512 (w), 1404 (s), 1053 (w), 1017 (w). UV/vis. (MeCN, λ_{max}, nm, ε $M^{-1}cm^{-1}$): 410 (1.42×10^3), 347 (8.62×10^3), 281 (8.70×10^3). Λ_M (MeOH, $ohm^{-1}cm^2mol^{-1}$): 54.

Preparation of $[Cu(H_2L1)_2]$ (3)

To a deprotonated solution of **H_3L1** [prepared by treatment of **H_3L1** (0.232 g, 1.0 mmol) with KOH (0.056 g, 1.0 mmol) in methanol (10 mL) under stirring over half an hour] methanolic solution (10 mL) of anhydrous $Cu(CH_3COO)_2$ (0.091 g, 0.5 mmol) was added drop wise and

reaction mixture allowed to stir for 4h at rt. Slowly green colored precipitate separated, which was collected by filtration washed with methanol and diethyl ether. Block shaped crystals were obtained by slow diffusion of diethyl ether over a dichloromethane solution of the complex within a couple of days. Yield based on **H_3L1** (0.181 g; 69%). Anal. Calcd. [$C_{28}H_{38}CuN_4O_2$]: C 63.91, H 7.28, N 10.65%, Found: C 63.86, H 7.19, N 10.53%. ESI-MS (Calcd., Found, *m/z*): 526.2424, 526.2360 [$(M+H)^+$, 18%]. IR (KBr pellets, cm^{-1}): 3455 (w), 3375 (w), 1626 (s), 1576 (s), 1514 (s), 1478 (w), 1400 (s), 1275 (w), 1120 (w), 1014 (m). UV/vis. (MeCN, λ_{max}, nm, ε $M^{-1}cm^{-1}$): 311 (7. 27 × 10^3), 289 (8.49 × 10^3).

X-ray structure determinations

Single crystal X-ray data on **H_3L1**, was collected on a R-AXIS RAPID II and for **1**, **2**, and **3** on a Bruker APEX II (kappa 4) diffractometer at room temperature with Mo-Kα radiation (λ = 0.71073 Å). Structures were solved by direct methods (SHELXS 97) and refined by full-matrix least squares on F^2 (SHELX 97).[2] All the non-H atoms were treated anisotropically. H atoms attached to the carbon were included as fixed contribution and were geometrically calculated and refined using the SHELX riding model. Computer program PLATON was used for analyzing the interaction and stacking distances.[3]

Result and discussion

^{1}H NMR Studies

The *enolic* –OH protons of **H_3L1**, **H_2L2** and **H_2L3** in their ^{1}H NMR spectra were displayed as a singlet at δ 11.87, 11.89 and 11.92 ppm, respectively ($CDCl_3$; Fig. S1-S3). Likewise, mesitylene ring and allylic protons also resonated as a singlet (δ 6.82 and 5.18, **H_3L1**; 6.99 and 5.22, **H_2L2**; 6.98 and 5.21 ppm, **H_2L3**). The integrated intensity and position of various signals clearly indicated condensation of only one amine unit with acetylacetone in **H_3L1**, while both the amines in **H_2L2**. Further, formation of **H_2L3** is strongly evidenced by the presence of a signal due to –CH=N– at δ 8.24 ppm and aromatic protons (four) associated with central phenylene ring at δ 8.03 ppm. The ^{13}C NMR spectra of **H_3L1**, **H_2L2** and **H_2L3** corroborated well with their ^{1}H NMR spectra and strongly supported formation of the respective ligands (Fig. S4-S6).

ESI-Mass Spectral Studies

The ESI-MS of **H_3L1**, **H_2L2** and **H_2L3** displayed molecular ion peaks $[M+H]^+$ at *m/z* 233.1657 (calcd. 233.1609, **H_3L1**), 315.2076 (calcd. 315.2028, **H_2L2**) and 563.3387 (calcd. 563.3341, **H_2L3**) (Fig. S7-S9) and strongly supported formation of the respective compounds. In its mass spectrum **1** displayed molecular ion peak at *m/z* 1239.2887 (calcd. 1239.2973) corresponding to $[M-3H]^+$. Prominent peaks assignable to half and one fourth unit of the cubane **1** at *m/z* 619.0770 and 310.2382 were also observable (Fig. S10). Likewise, ESI-MS of **2** exhibited molecular ion peak at *m/z* 1239.2827 $[M+H]^+$ (calcd. 1239.2973) along with two other peaks at *m/z* 619.1339 and 310.0699 due to half and one fourth units of the cubane (Fig. S11). Isotopic abundance pattern of the molecular ion peaks in **1** and **2** matched well with the calculated one (Fig. S12). On the other hand, mononuclear complex **3** displayed molecular ion peak $[M+H]^+$ at *m/z* 526.2360 (calcd. 526.2424) which also matched with calculated isotopic pattern (Fig. S13-S14). Overall ESI-Mass spectral pattern is consistent with the formulation of **H_3L1**, **H_2L2** and **H_2L3**, tetranuclear cubanes **1**, **2** and mononuclear complex **3**.

Absorption and emission Studies

The electronic absorption spectra of **H_3L1**, **H_2L2**, and **H_2L3** (c, 100 μM, MeCN) at room temperature exhibited strong absorptions due to intra-ligand charge transfer transitions in the high energy region (**H_3L1**, 307; **H_2L2**, 309; **H_2L3**, 303 nm; Fig. S15, ESI†). Cubane **1** exhibited a strong low energy band at ~430 nm and **2** a weak one at ~410 nm attributable to ligand to metal charge transfer (LMCT) transitions. In addition, **1** and **2** displayed another band at ~349 nm and ~347 nm, respectively (Table S5). Complex **3** exhibited two bands at 311 and 290 nm associated with ligand based transitions (Fig. S15, ESI†). Due to symmetrical nature **1** did not show any band in its CD spectra (Fig. S16, ESI†).

Generally, copper complexes are non fluorescent due to paramagnetic nature of the Cu(II). Cubane **1** shows weak fluorescence, while **2** is almost non fluorescent in nature. Upon excitation at 410 nm **1** displayed a band at 504 nm with quantum yields (Φ) of 0.07 (**1**) while **2** shows very weak band at 499 nm. The greater fluorescence in **1** relative to **2** may be attributed to presence of the NH_2^+ group. It was further supported by addition of four equiv of 0.1M HNO_3 to a solution of **2** that leads to a significant fluorescence enhancement that is almost comparable to **1** (Fig. S17, ESI†). The conductance measurement in methanol supported the ionic nature of cubane **1** as 4:1 electrolyte while **2** is charge neutral species.[4]

Electrochemical Studies

The redox properties of **H_3L1**, **H_2L2**, **H_2L3** and **1-3** have been investigated by cyclic voltammograms (CV) and differential pulse voltammograms (DPV) under nitrogen atmosphere at room temperature in the potential range +2.0 to –2.0 V, (MeCN, c = 100 μM) (Fig. S18-S21, Table S6-S7, ESI†). In their CV the ligands exhibited an irreversible oxidative wave at E*pa* 0.520, **H_3L1**; 0.525, **H_2L2** and 0.518 V, **H_2L3** (Fig. S18, ESI†) in the anodic potential window while no wave appeared in the cathodic window. Cubanes **1** and **2** displayed irreversible wave in the anodic region at E*pa* 0.559; **1**, 0.563; **2**, and reduction waves at −0.896 and 0.909 V corresponding to $Cu^{2+} \rightarrow Cu^{+}$ redox couple (Fig. S19-S20, ESI†).[5] Since all the four copper centers in **1** and **2** are identical, hence in their cyclic voltmmograms these displayed only a single reduction wave. On the other hand, mononuclear complex **3** displayed irreversible oxidation wave at E*pa* 0.536, and reduction wave at −0.691 V due to $Cu^{2+} \rightarrow Cu^{+}$ (Fig. S21, ESI†), Analogous conclusions has also been drawn on these systems from DPV (Table S7, ESI†).

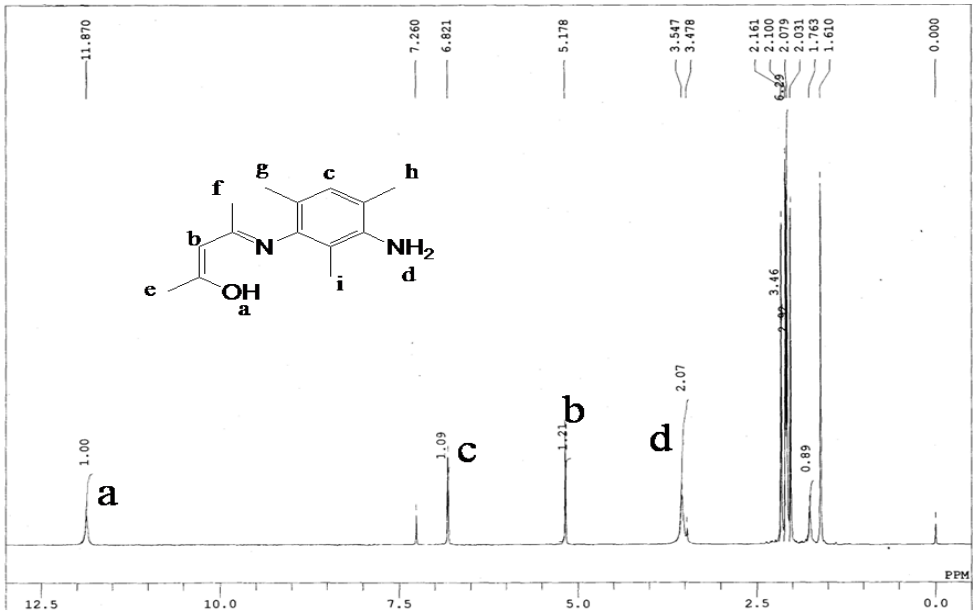

Fig. S1 ^{1}H NMR spectrum of $\mathbf{H_3L1}$.

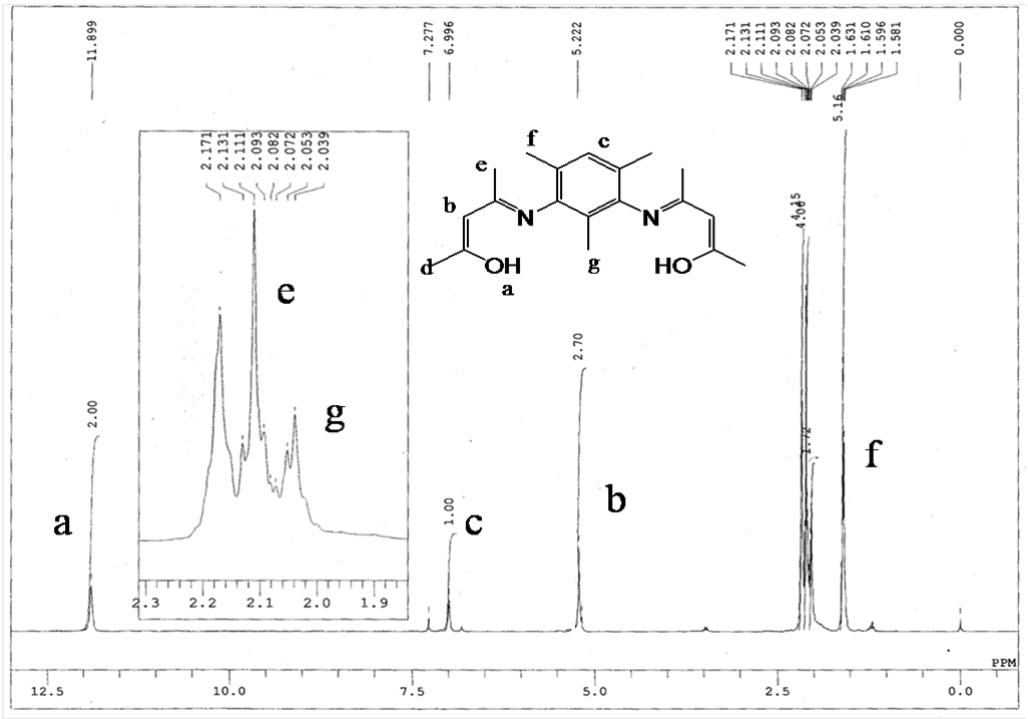

Fig. S2 ^{1}H NMR spectrum of $\mathbf{H_2L2}$.

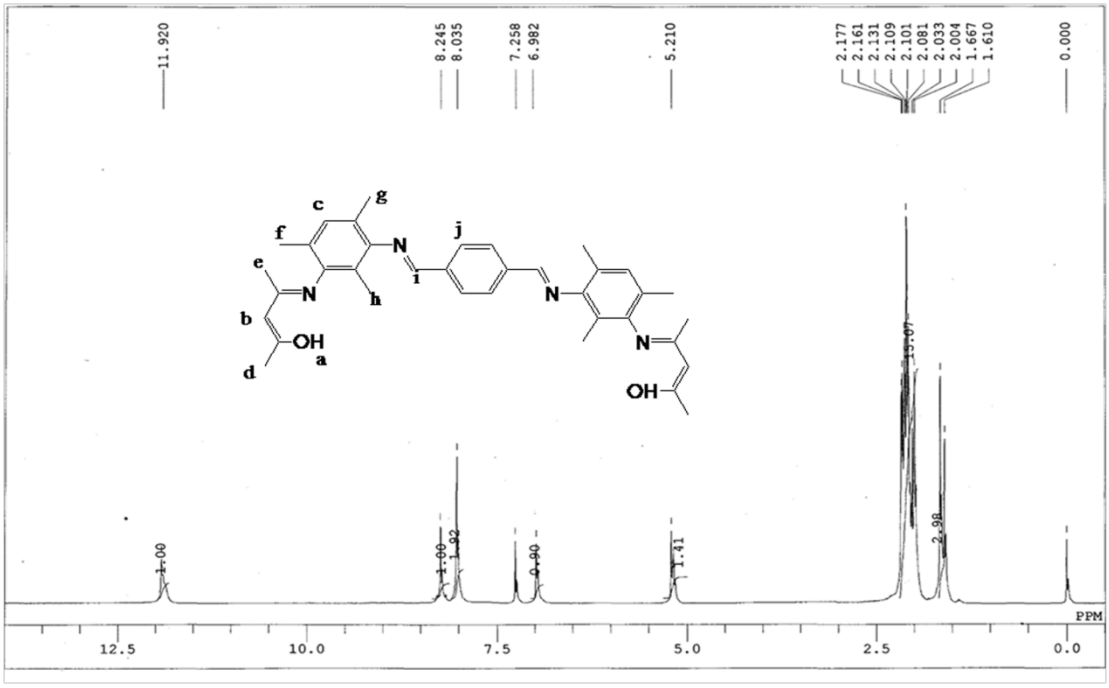

Fig. S3 ^{1}H NMR spectrum of **H_2L3**.

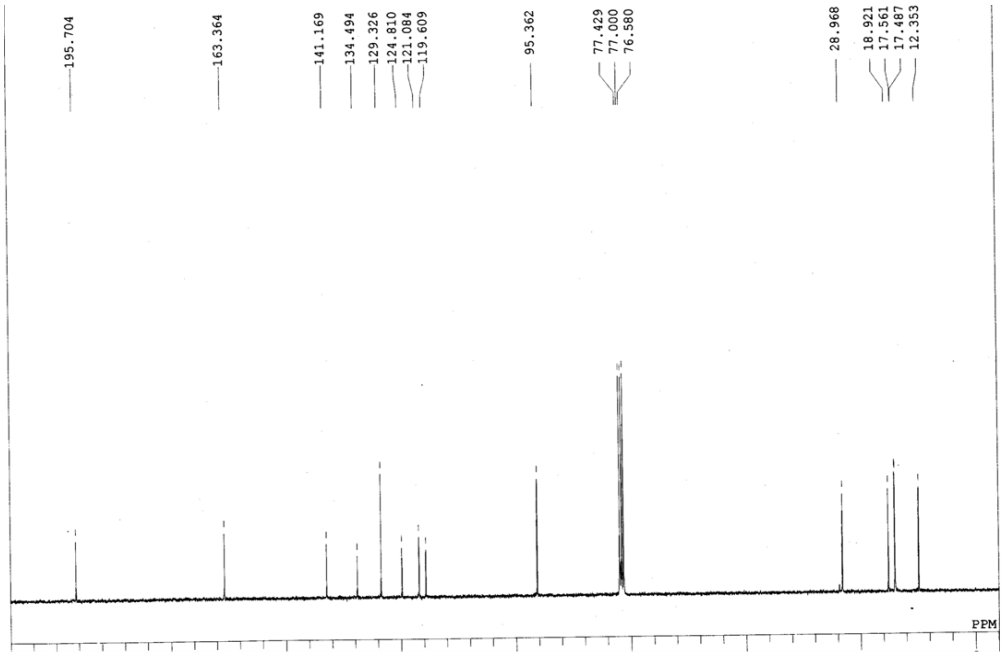

Fig. S4 ^{13}C NMR spectrum of **H_3L1**.

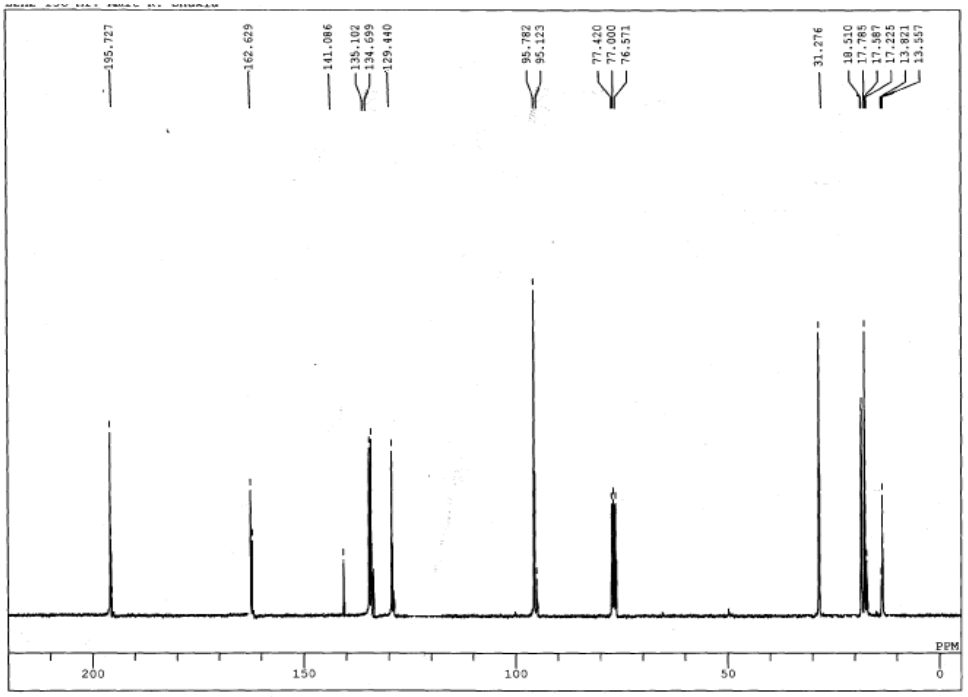

Fig. S5 ^{13}C NMR spectrum of **H_2L2**.

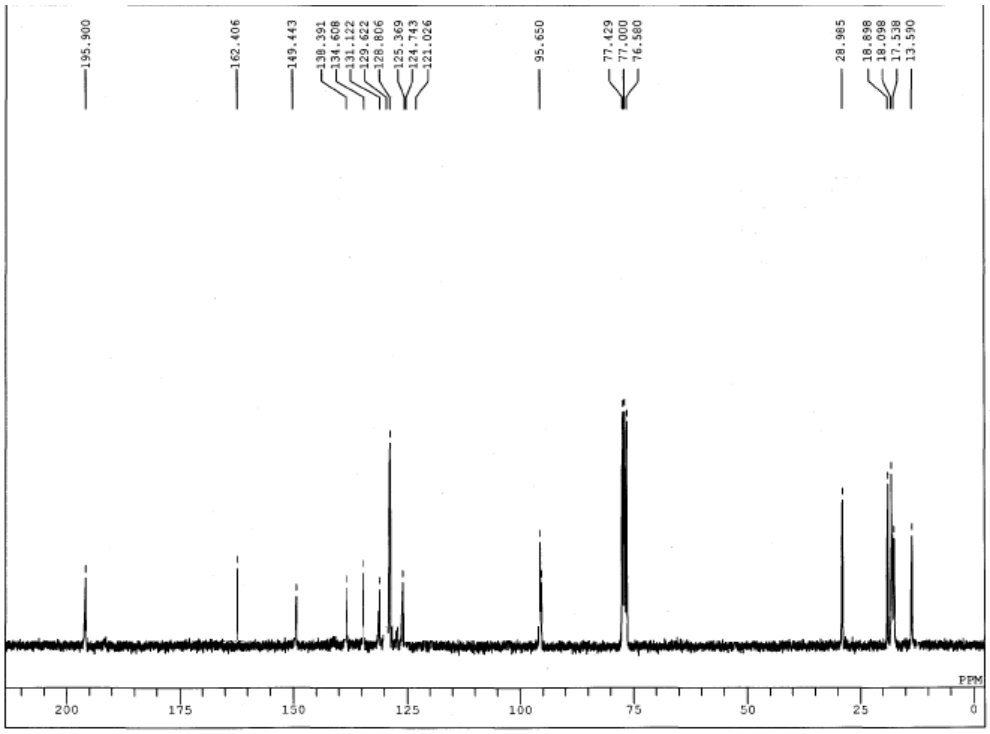

Fig. S6 ^{13}C NMR spectrum of **H_2L3**.

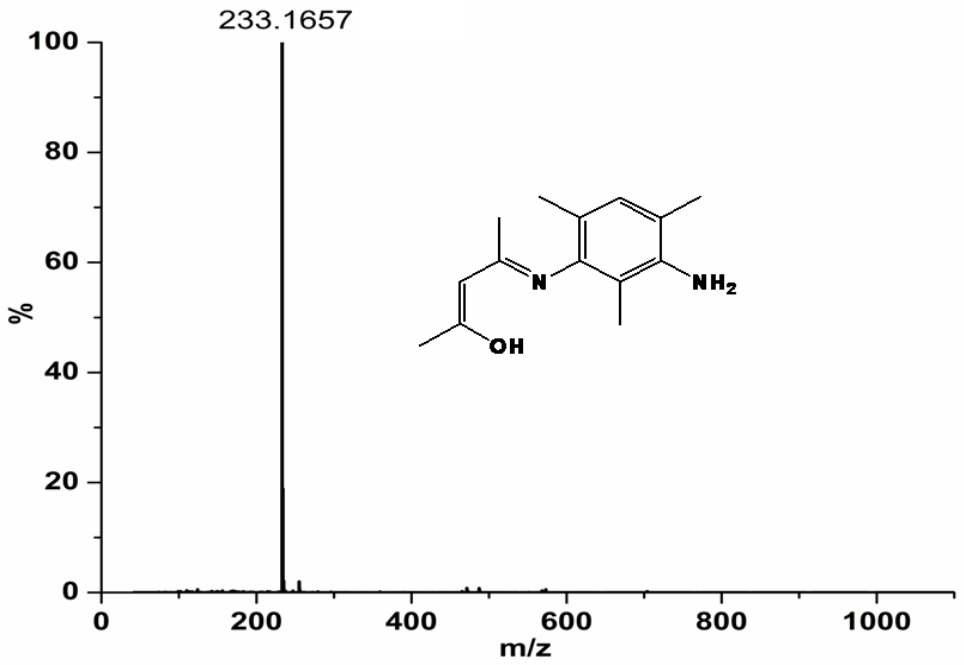

Fig.S7 ESI-Mass spectrum of **H_3L1**.

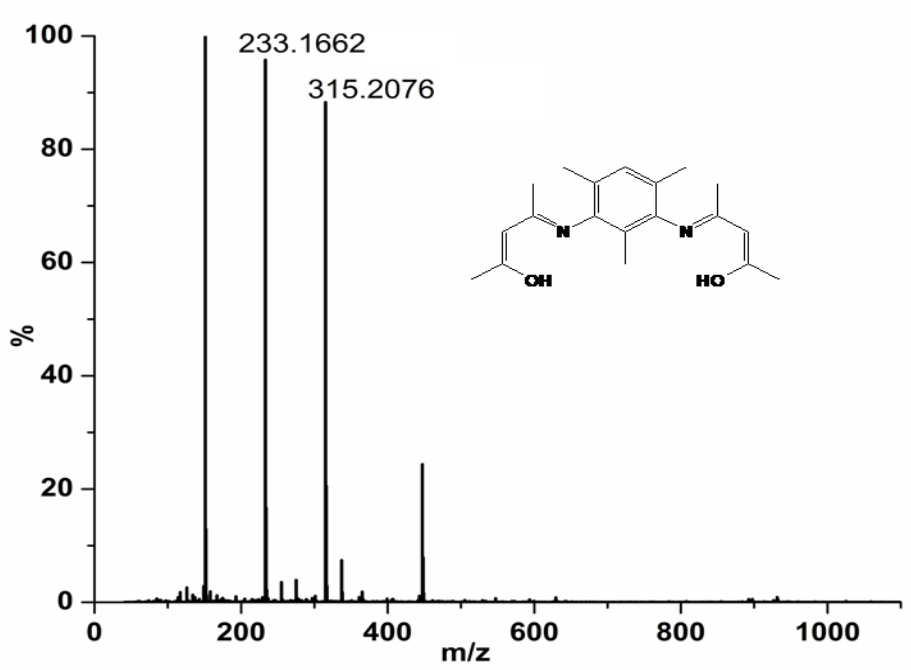

Fig. S8 ESI-Mass spectrum of **H_2L2**.

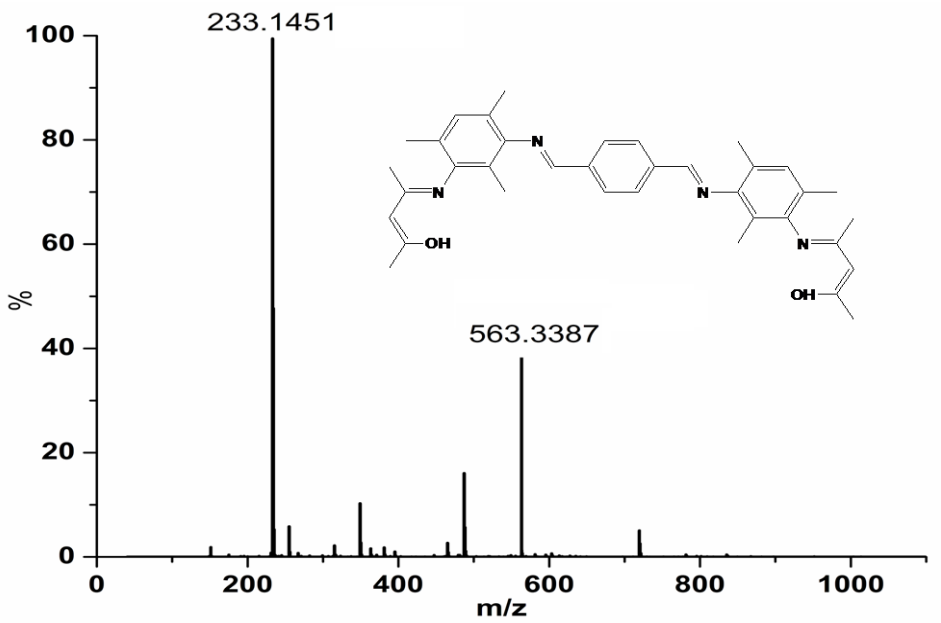

Fig. S9 ESI-Mass spectrum of $\mathbf{H_2L3}$.

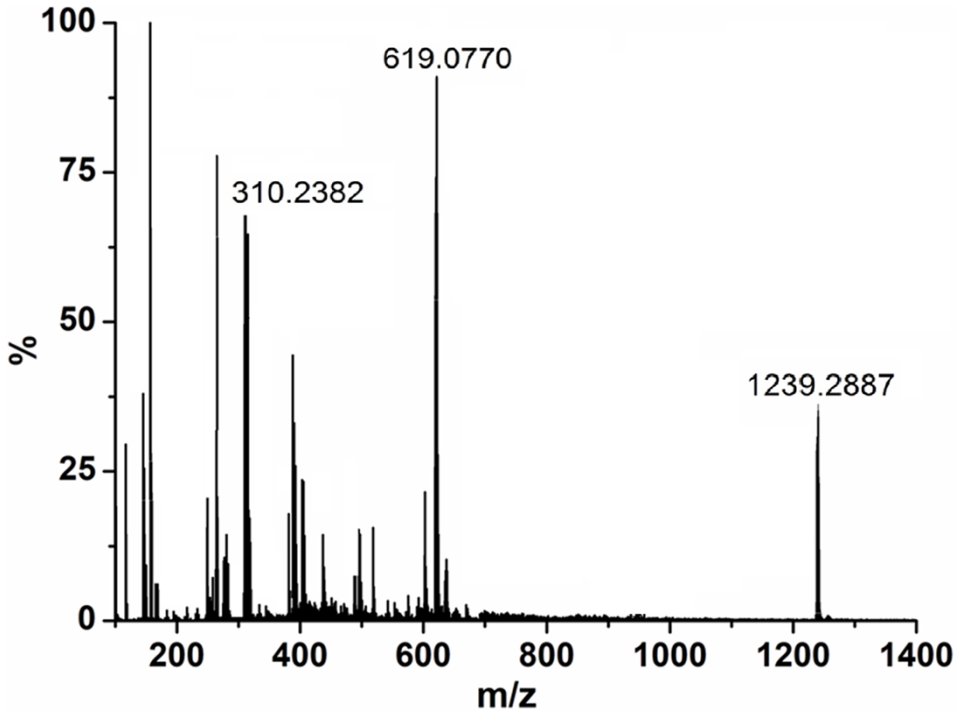

Fig. S10 ESI-Mass spectrum of **1**.

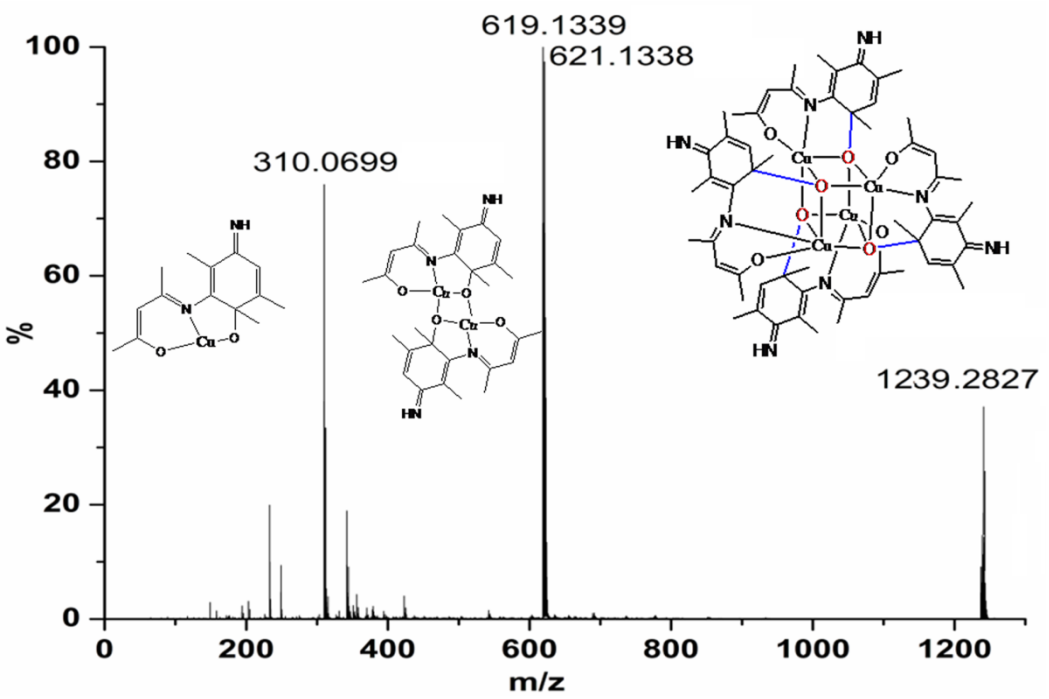

Fig. S11 ESI-Mass spectrum of **2**.

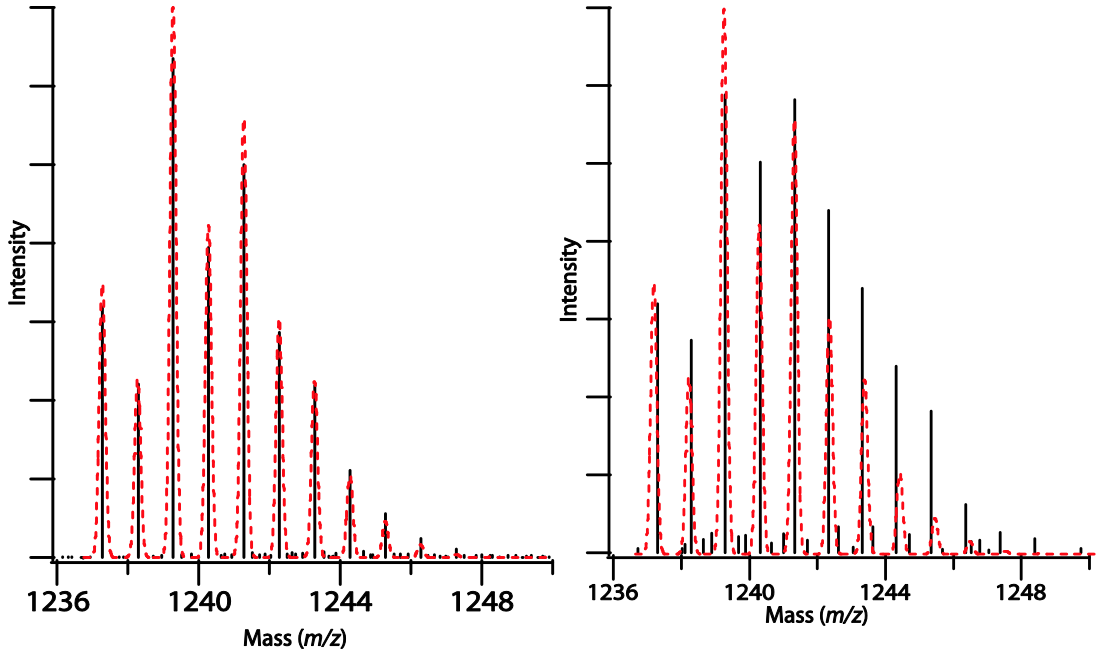

(a) (b)

Fig. S12 Simulated isotopic pattern in ESI-Mass spectrum of **1** at *m/z* 1239.2887 (a), and **2** at *m/z* 1239.2827 (b); calculated (black) and experimental (red).

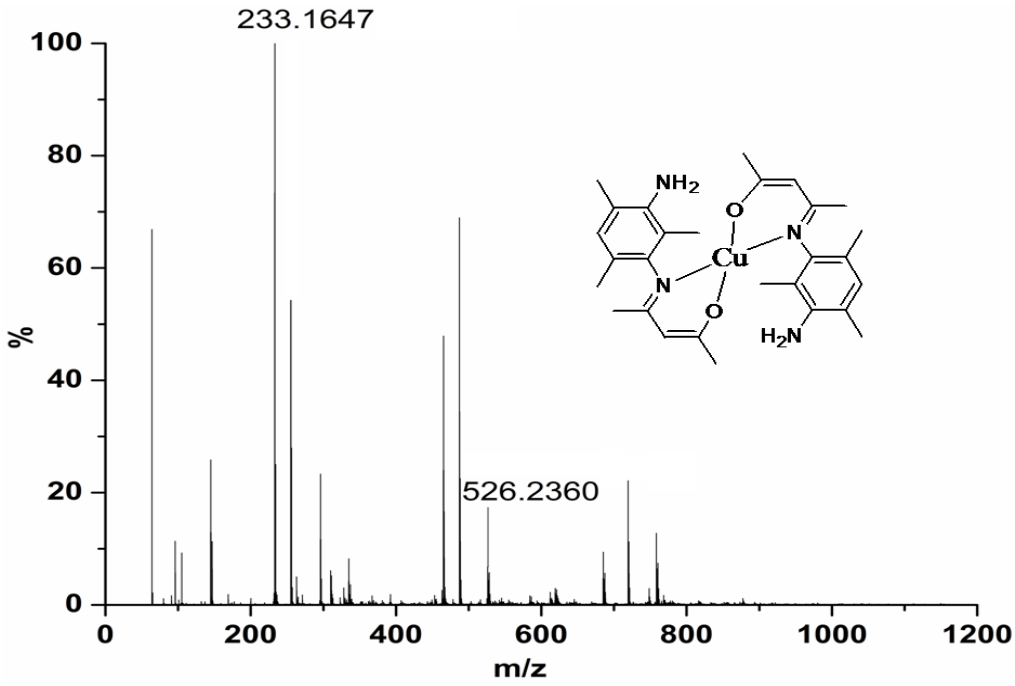

Fig. S13 ESI-Mass spectrum of **3**.

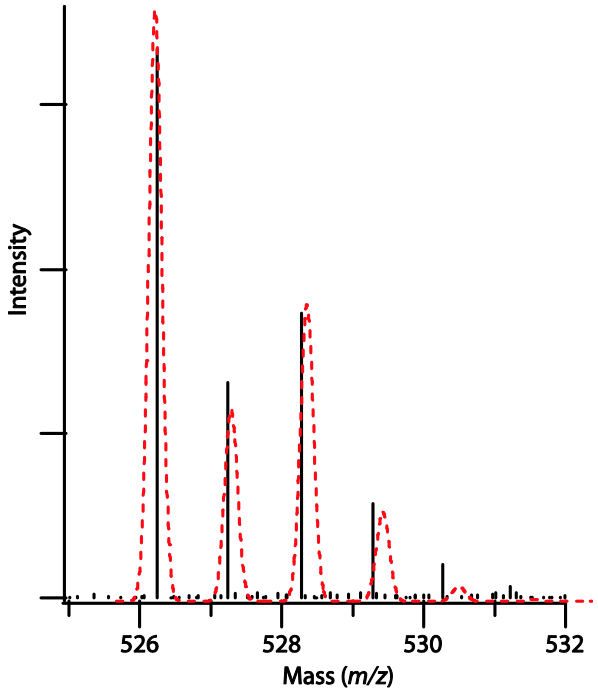

Fig. S14 Simulated isotopic pattern for ESI-Mass spectrum of **3** (*m/z* 526.2360); calculated (black) and experimental (red).

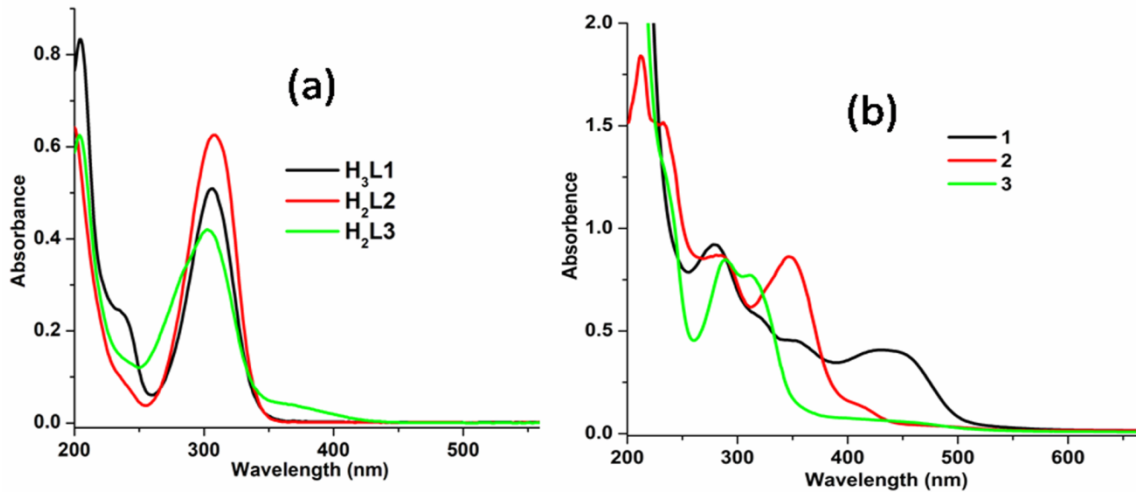

Fig. S15 UV/vis spectra of **H_3L1**, **H_2L2**, **H_2L3** (a) and **1-3** (b) in MeCN (c, 100 μM).

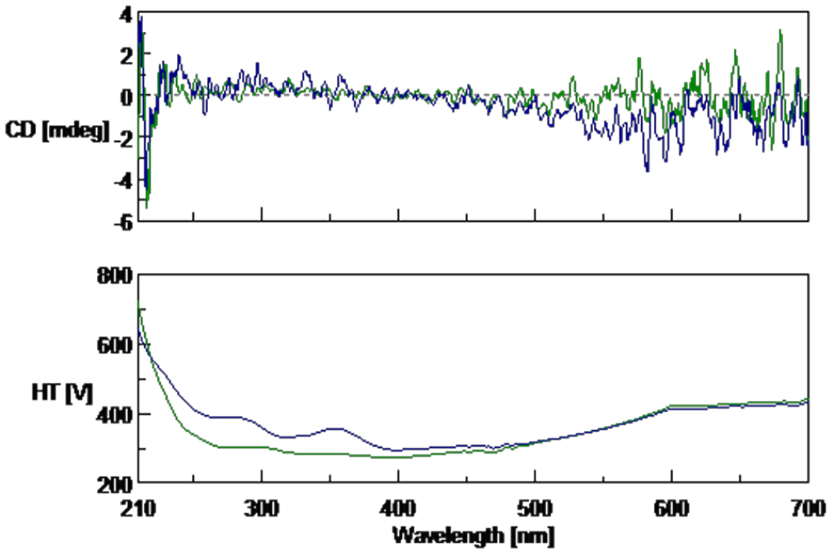

Fig. S16 UV/vis (bottom) and CD (top) spectra of **1**.

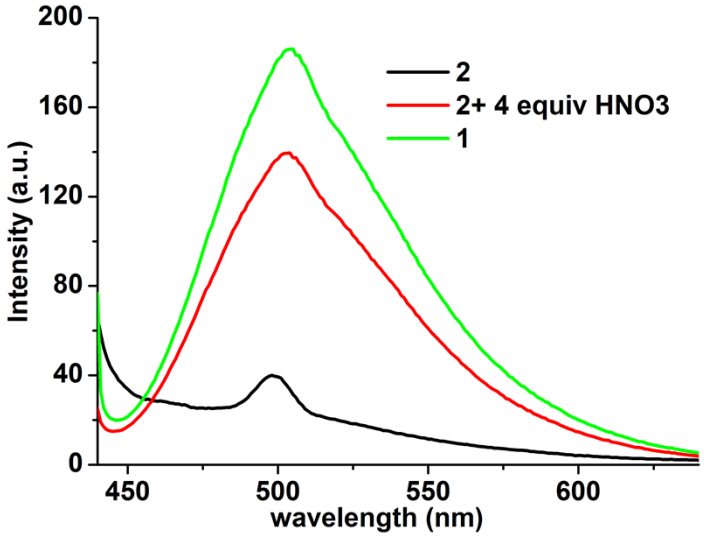

Fig. S17 Emission spectra of cubane **1** (green), **2** (black) and **2** + HNO_3 (4 equiv. ; red).

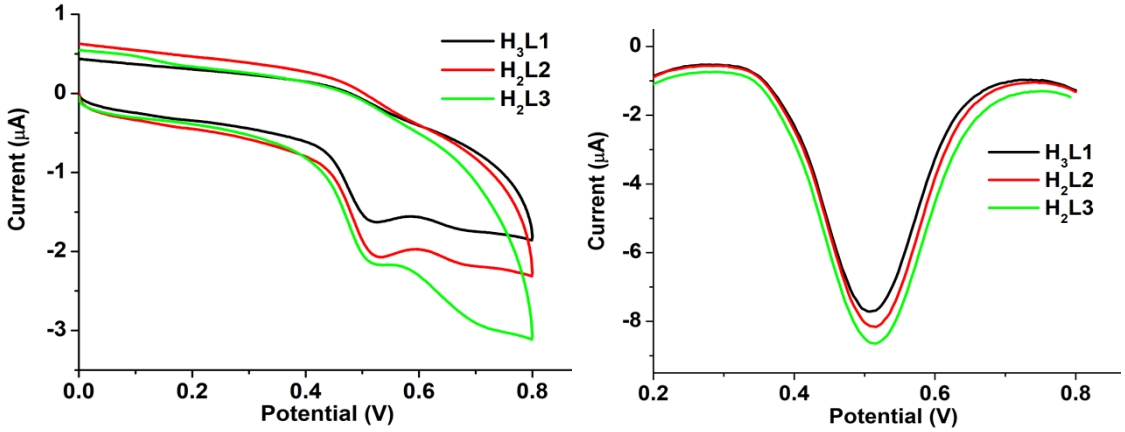

(a) (b)

Fig. S18 Cyclic (a), and differential pulse voltammograms (b) for **H_3L1**, **H_2L2**, **H_2L3** in MeCN (c = 100 μM).

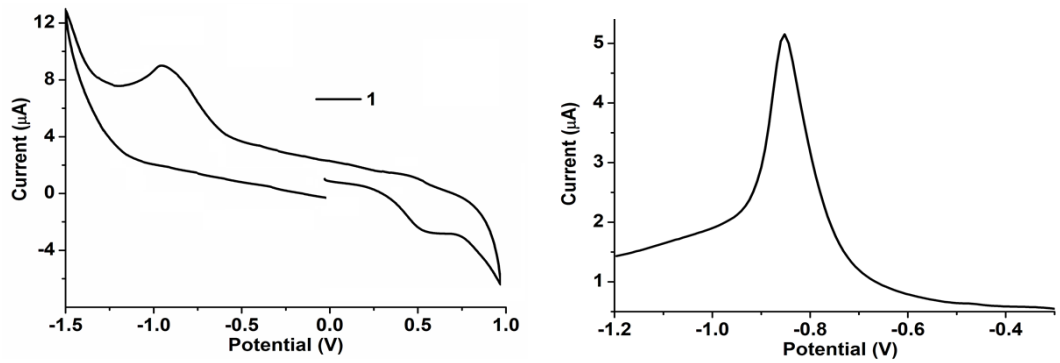

(a) (b)

Fig. S19 Cyclic (a) and differential pulse voltammograms (b) for **1** in MeCN (c, 100 μM).

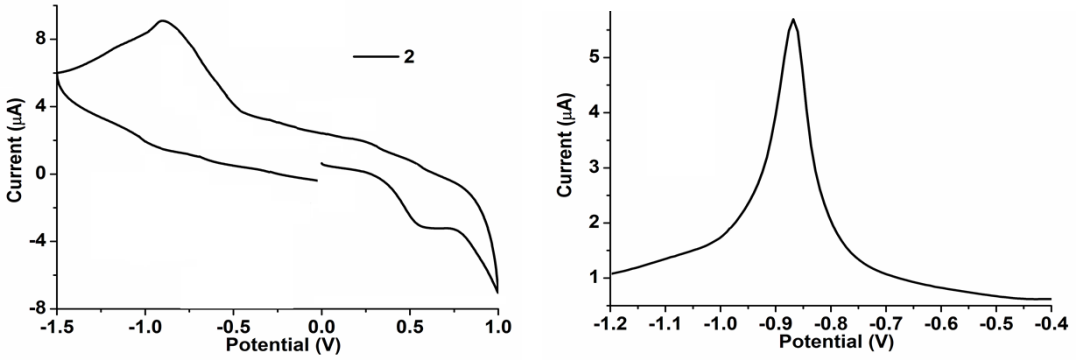

(a) (b)

Fig. S20 Cyclic (a) and differential pulse voltammograms (b) for **2** in MeCN (c, 100 μM).

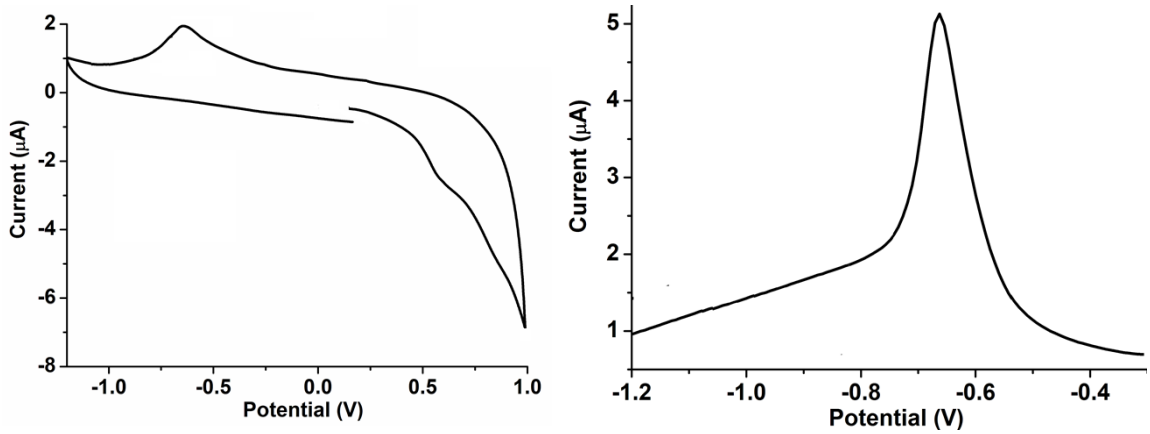

(a) (b)

Fig. S21 Cyclic (a) and differential pulse voltammograms (b) for **3** in MeCN (c, 100 μM).

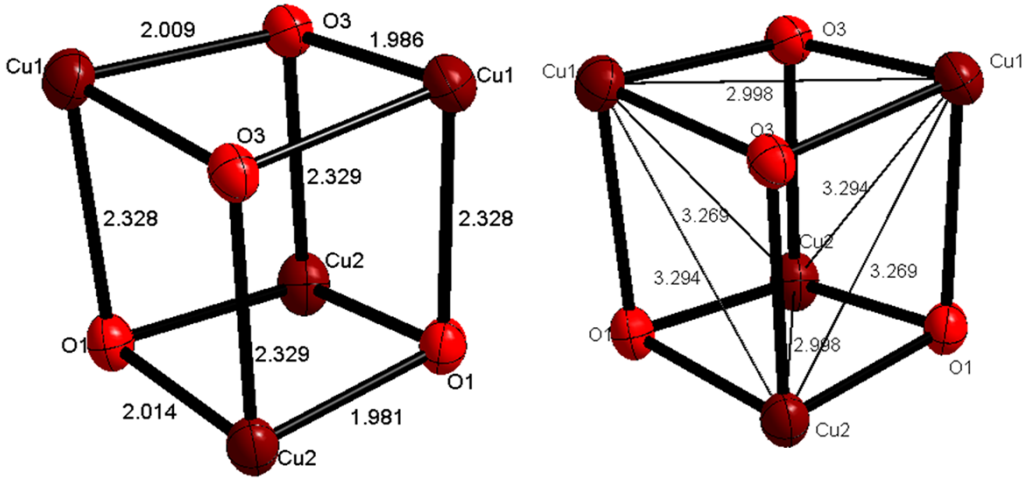

Fig. S22 Cu_4O_4 cubane core showing Cu–O and Cu–Cu distances in **2**.

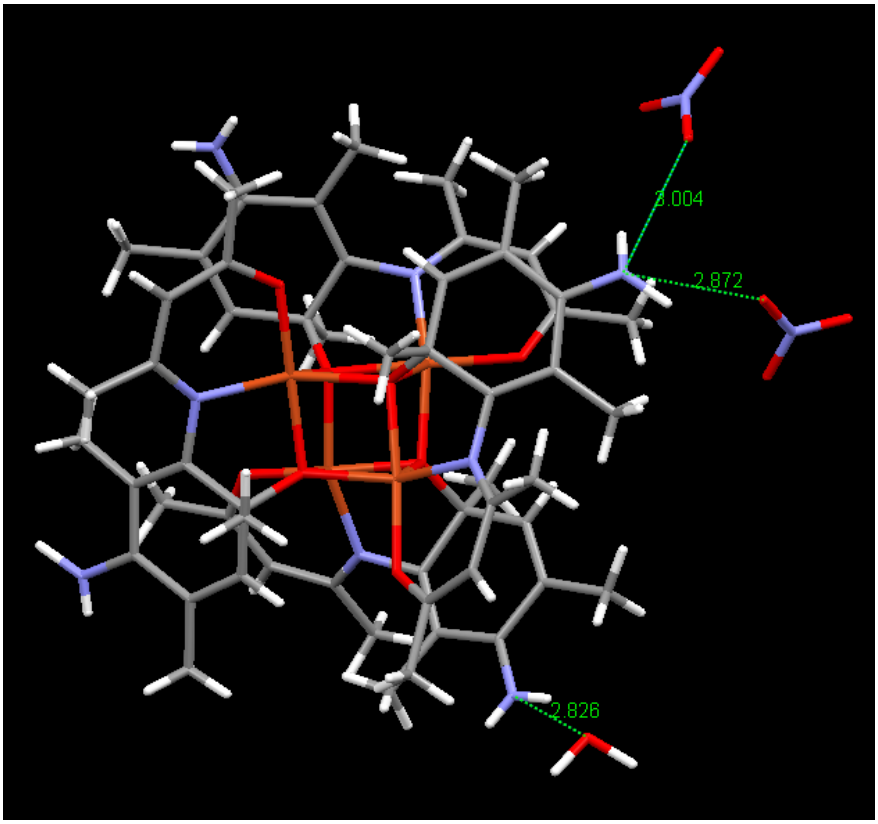

Fig. S23 Hydrogen bonding interactions between one $=NH_2^+$ (N4) and oxygen atoms from two nitrates (N4–H4A/4B···O9; 2.872/3.004) and other $=NH_2^+$ (N2) with water (N2–H2A···O11; 2.826) in **1**.

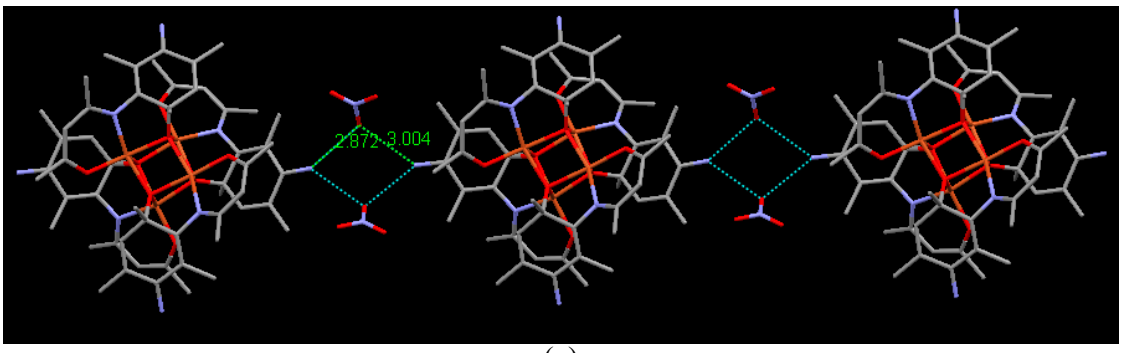

(a)

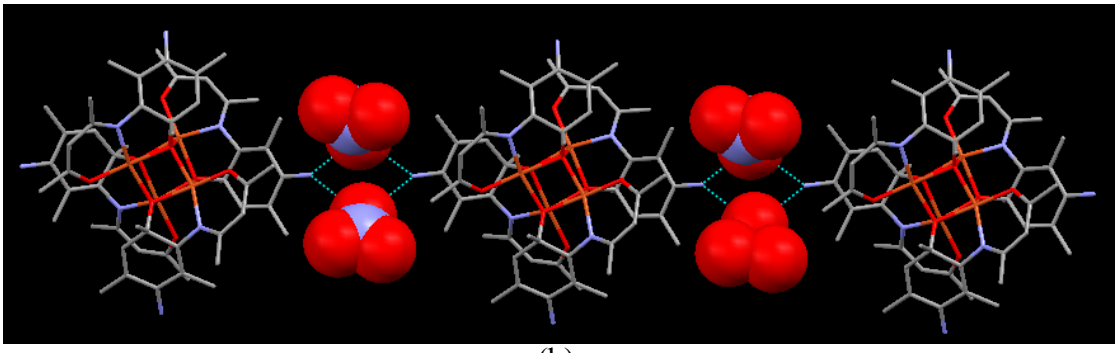

(b)

Fig. S24 Hydrogen bonding interactions between $=NH_2^+$ (N4) and oxygen from the nitrates (N4–H4A/4B···O9) resulting in a rectangular cavity in **1**.

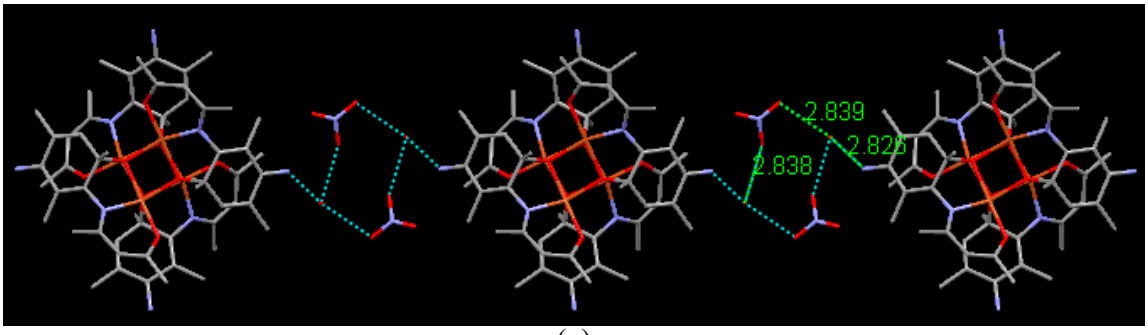

(a)

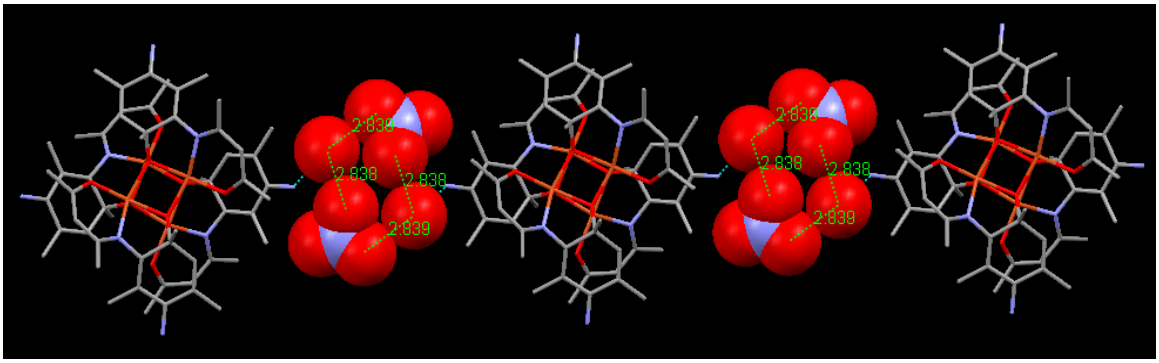

(b)

Fig. S25 Hydrogen bonding interactions between $=NH_2^+$ (N2) and oxygen from water and nitrates (N2–H2A···O11) in **1**.

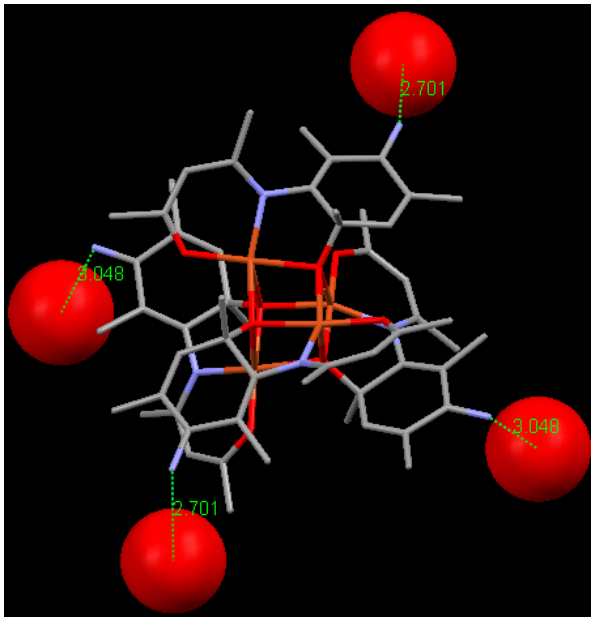

(a)

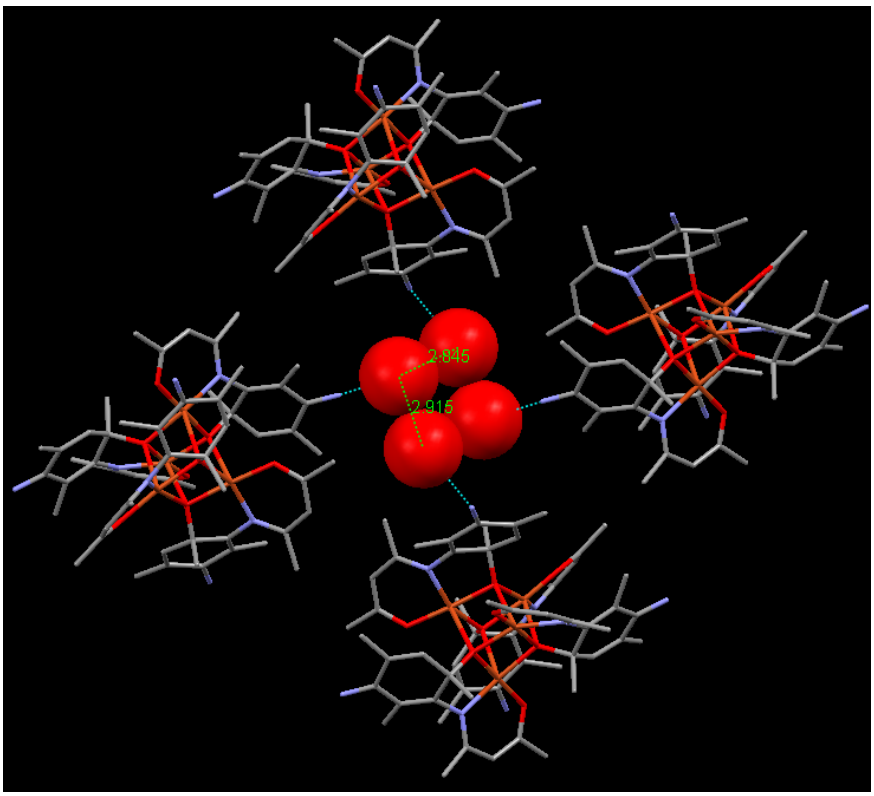

(b)

Fig. S26 Hydrogen bonding interactions between =NH with water (N2–H2···O11/ N4–H4···O12; 2.701/3.048 Å), (a) and arrangment of water molecules in rectangle environment (b) in **2**.

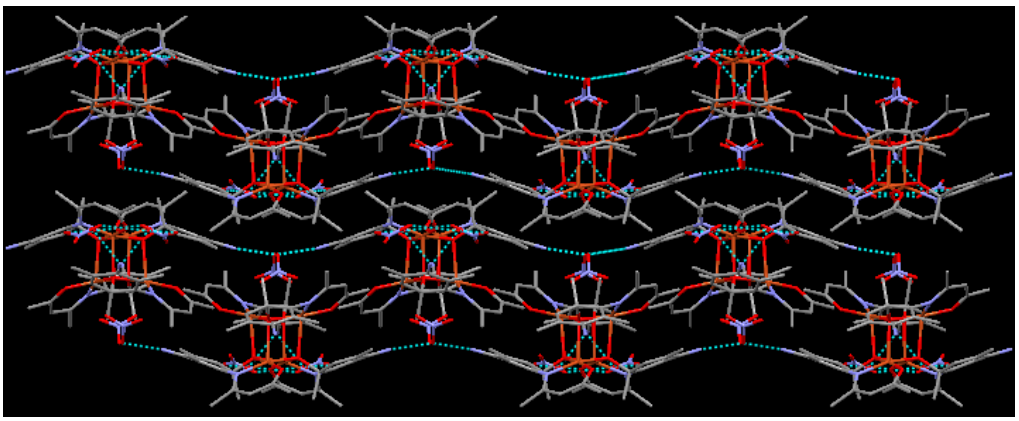

Fig. S27 Helical structure resulting from hydrogen bonding between $=NH_2^+$ with oxygen of the nitrates and water along c axis in **1**.

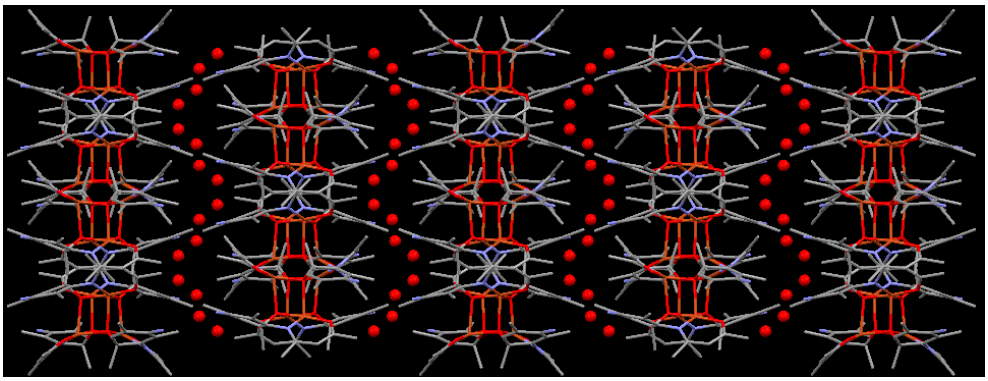

Fig. S28 Helical arrangement of water molecules in **2** through hydrogen bonding interactions.

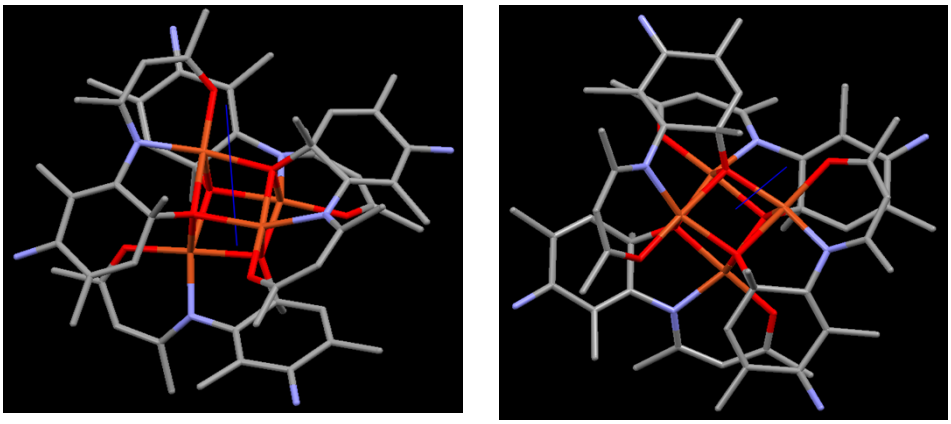

Fig. S29 Symmetric C_2 axis passing through cubane center of **1** and **2**.

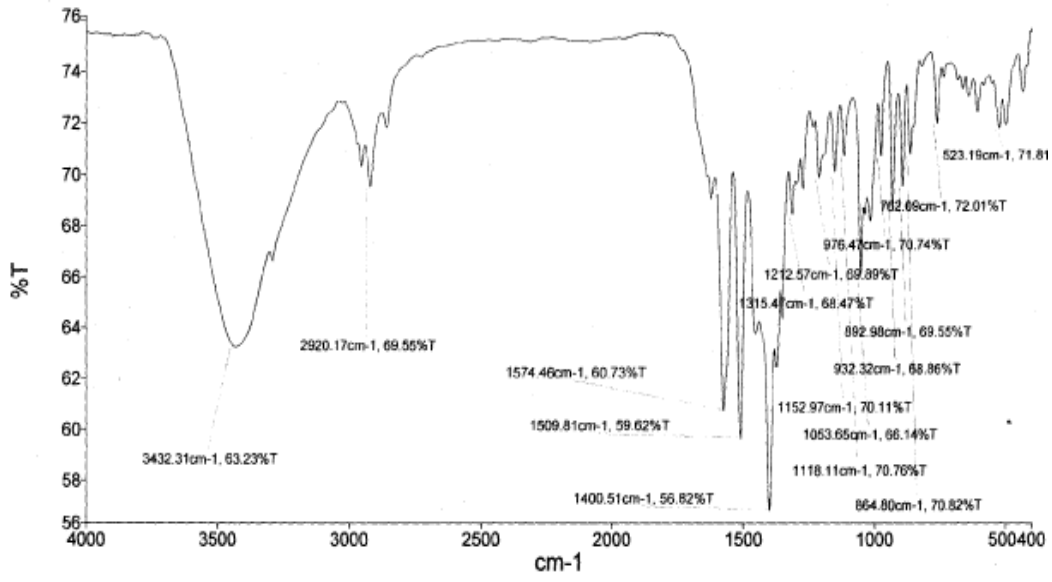

Fig. S30 IR spectra of the Co complex with **H_3L1**.

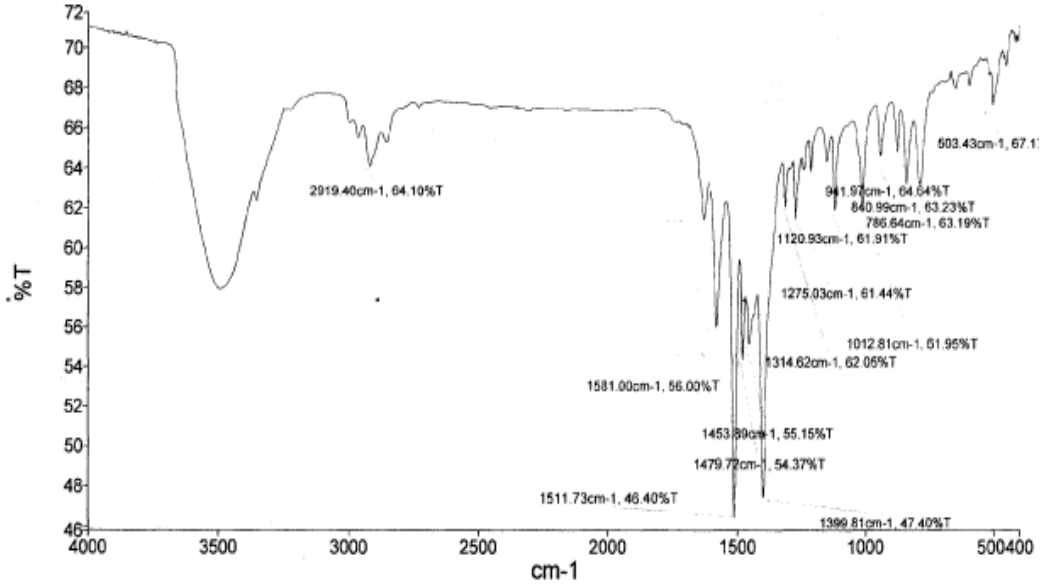

Fig. S31 IR spectra of the Ni complex with **H_3L1**.

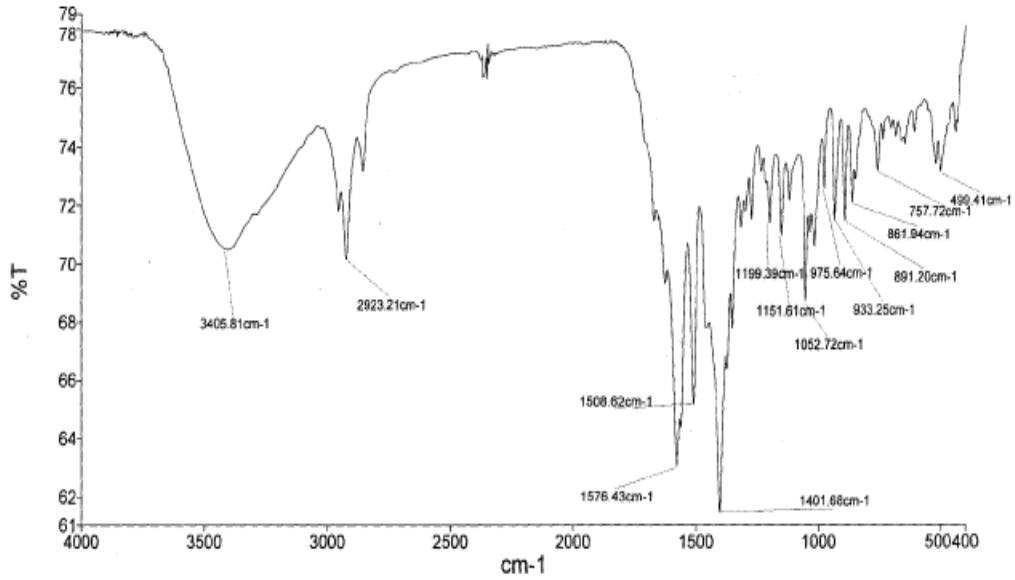

Fig. S32 IR spectra of the Mn complex with **H_3L1**.

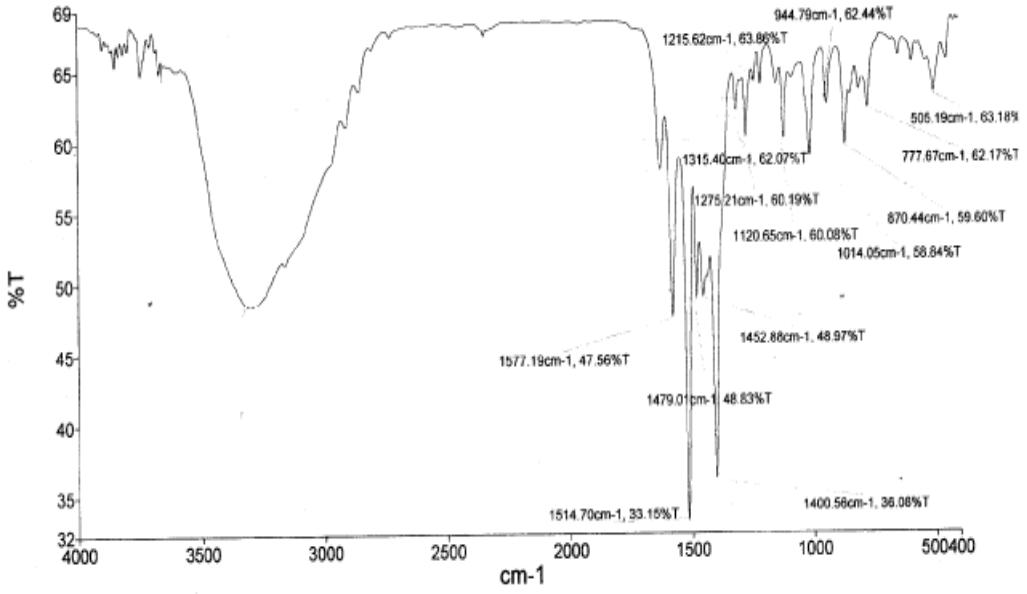

Fig. S33 IR spectra of the Zn complex with **H_3L1**.

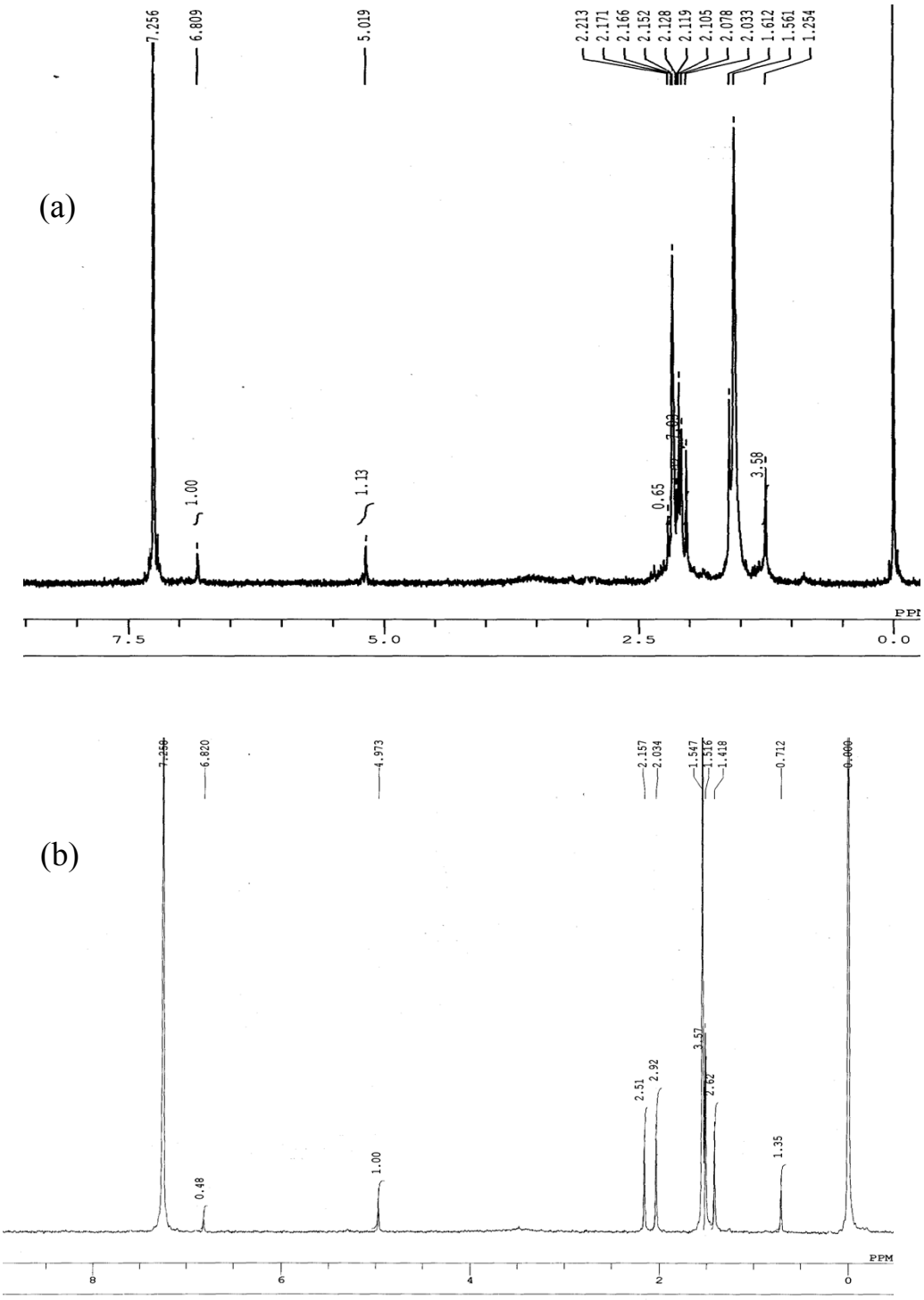

Fig. S34 ^{1}H NMR spectra for the Zn complexes [derived from **H_3L1**; $Zn(H_2L1)_2$ (a), and **H_2L2**; $(ZnL2)_2$, (b)] showing lack of any transformation in the ligands.

Qualitative Analysis Report

Data Filename	acdsp.d	**Sample Name**	acdsp
Sample Type	Sample	**Position**	Vial 11
Instrument Name	Instrument 1	**User Name**	CBMR-PC\admin
Acq Method	Direct Mass.m	**Acquired Time**	6/19/2014 12:04:09 PM
IRM Calibration Status	Success	**DA Method**	Regular.m
Comment	+ VE MODE		

Acquisition SW Version 6200 series TOF/6500 series Q-TOF B.05.00 (B5042.0)

User Chromatograms

Fragmentor Voltage 100 **Collision Energy** 0 **Ionization Mode** ESI

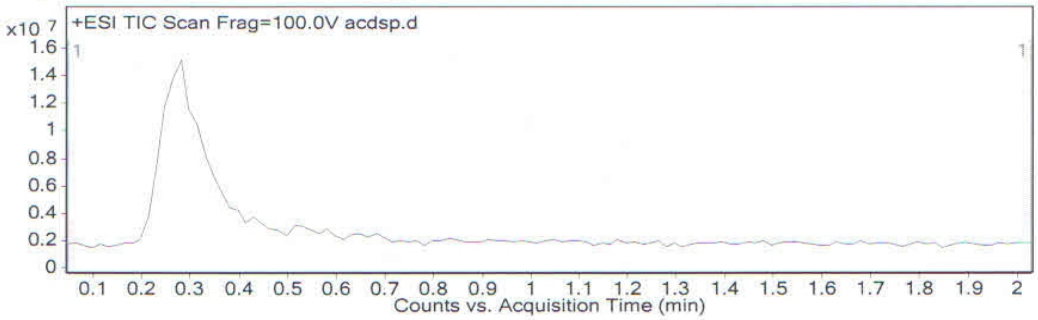

User Spectra

Fragmentor Voltage 100 **Collision Energy** 0 **Ionization Mode** ESI

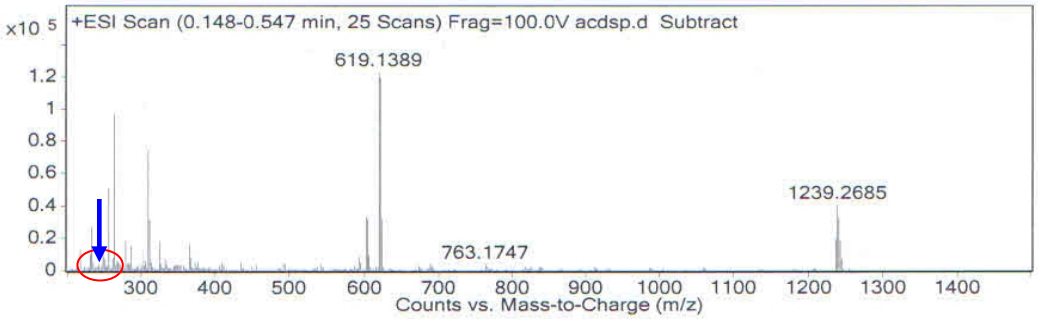

Peak List

m/z	z	Abund
81.0317	1	109358.8
172.0939	1	56430.2
255.1461	1	51002.06
263.1749	1	96841.38
310.0733	1	74415.69
619.1389	1	122979.52
620.1393	1	44993.65
621.1374	1	119206.97
622.1377	1	40958.76
1239.2685	1	40238.22

Fig. S35 HRMS of mother liquid in full range showing a feeble peak for **H3L1O⁻** (blue arrow in red circle).

Qualitative Analysis Report

Data Filename	acdsp.d	**Sample Name**	acdsp
Sample Type	Sample	**Position**	Vial 11
Instrument Name	Instrument 1	**User Name**	CBMR-PC\admin
Acq Method	Direct Mass.m	**Acquired Time**	6/19/2014 12:04:09 PM
IRM Calibration Status	Success	**DA Method**	Regular.m
Comment	+ VE MODE		

Acquisition SW Version 6200 series TOF/6500 series Q-TOF B.05.00 (B5042.0)

User Chromatograms

Fragmentor Voltage 100 **Collision Energy** 0 **Ionization Mode** ESI

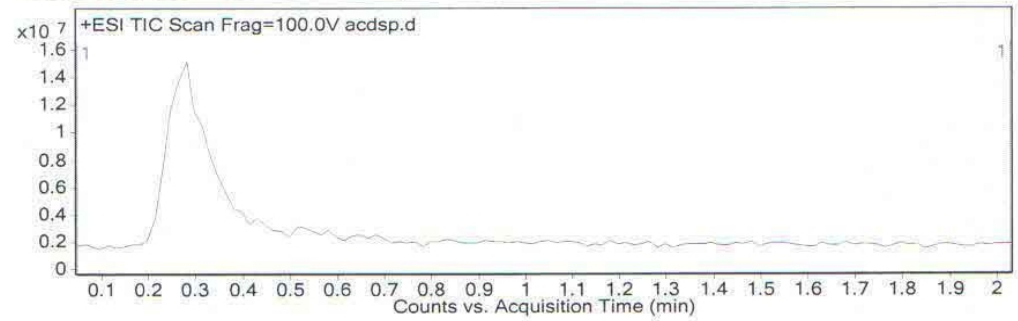

User Spectra

Fragmentor Voltage 100 **Collision Energy** 0 **Ionization Mode** ESI

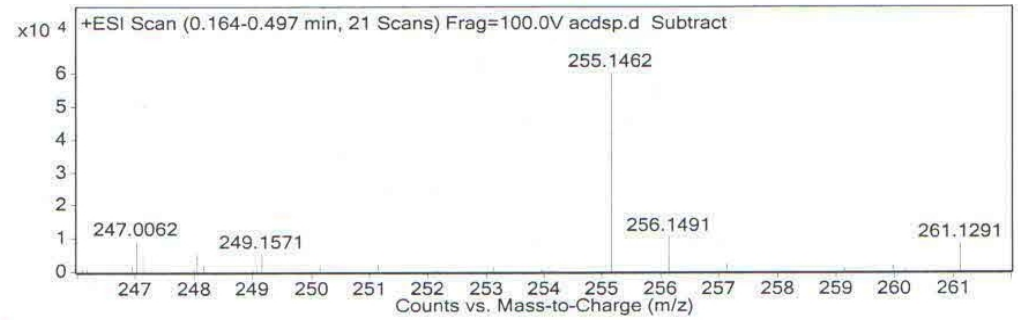

Peak List

m/z	z	Abund
76.998	1	38369.2
81.0317	1	113168
107.967	1	9790.54
172.0939	1	56084.39
185.1141	1	19344.14
217.1036	1	14318.97
231.1482	1	13217.47
233.1639	1	30860.98
255.1462	1	60077.22
256.1491	1	10297.96
263.1749	1	114955.7
264.1777	1	19667.74
279.1697	1	22524.22
286.1412	1	17844.71

Fig. S36 HRMS of mother liquid in specific range for **H_3L1O**.

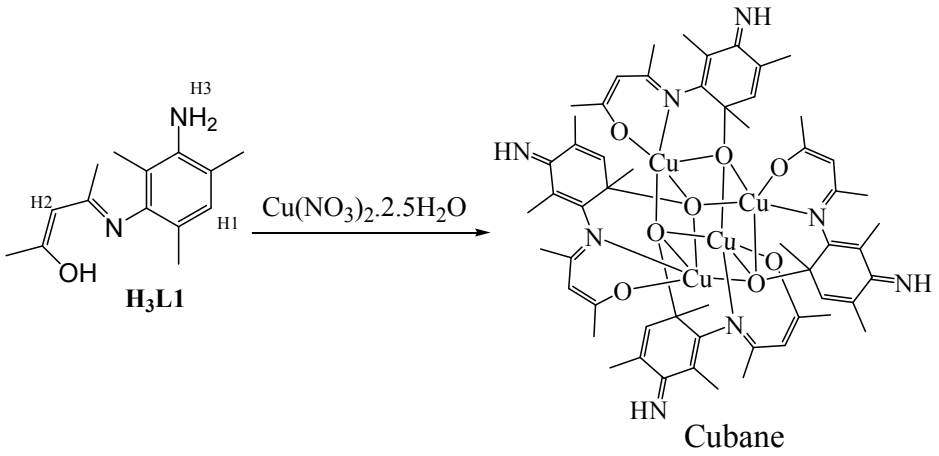

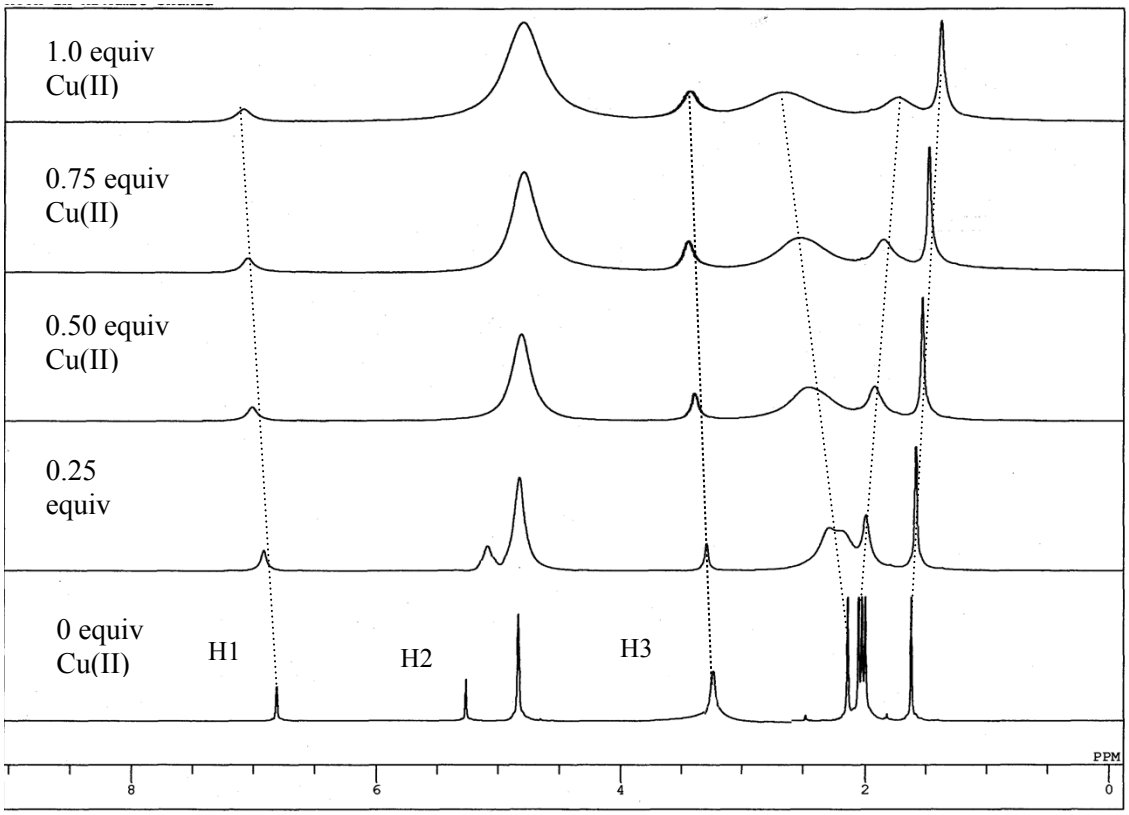

Fig. S37 ^{1}H NMR titration of **H_3L1** (CD_3OD) vs. Cu(II) nitrate in D_2O showing spectral changes involved in the formation of **1**. Aromatic proton H1 shifted toward down field while allylic proton upfield side and methyl protons broadened and shifted towards both upfield and down filed region. The results show complete disruption of the aromaticity of **H_3L1**. Amine protons (H3) may be merged with the solvent peak at 3.80 ppm. No peak corresponding to **H_3L1O** appeared in the spectra which suggested immediate complexation of the oxidized species with metal and discard the free existence of **H_3L1O**.

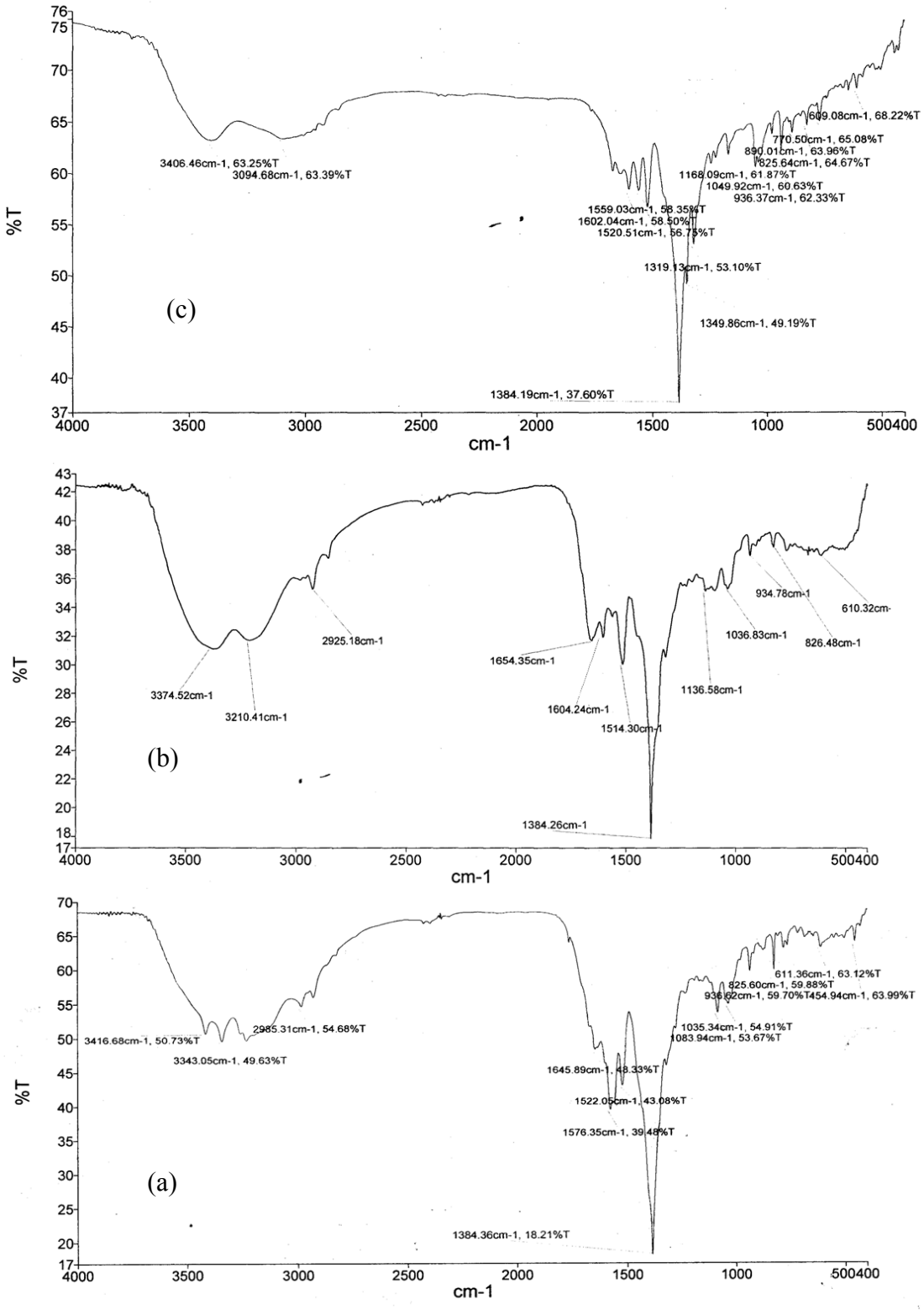

Fig. S38 IR Spectra of the product from reaction between **H_3L1** and $Cu(NO_3)_2.2.5H_2O$ in presence of MeOH/KOH (a), dry CH_3CN/NaH (b) and dry CH_3CN/NaH under nitrogen atmosphere (c).

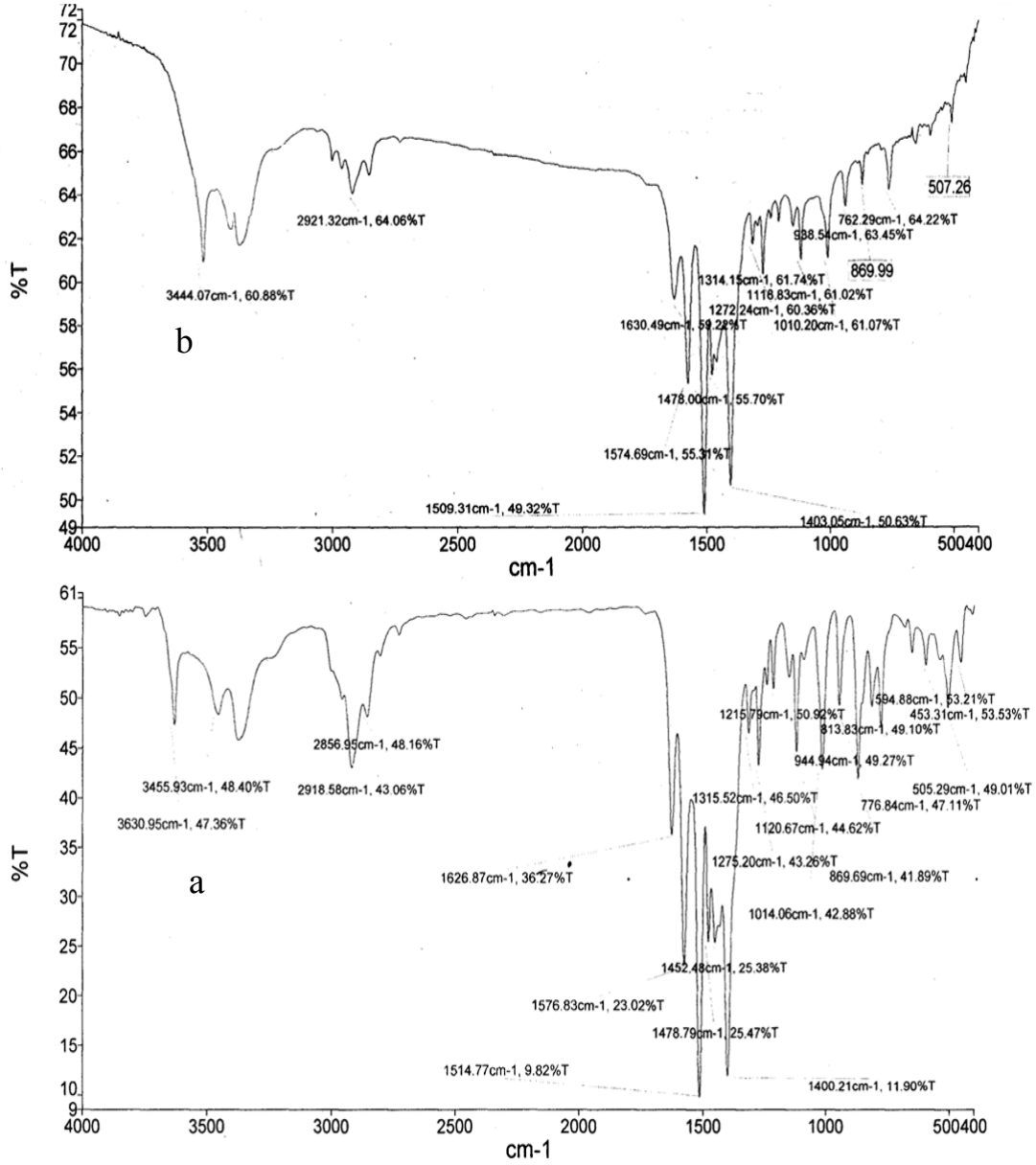

Fig. S39 IR Spectra of **3** synthesized using MeOH/KOH (a) and dry CH_3CN/NaH (b).

Table S1 Crystallographic parameter of **H_3L1**, **1**a-c, **2** and **3**

	H_3L1	**1a**	**1b**	**1c**	**2**	**3**
empirical formula	$C_{14}H_{20}N_2O$	$C_{56}H_{80}Cu_4N_{12}O_{22}$	$C_{56}H_{80}Cu_4N_{12}O_{22}$	$C_{56}H_{80}Cu_4N_{12}O_{22}$	$C_{56}H_{72}Cu_4N_8O_{12}$	$C_{28}H_{38}CuN_4O_2$
formula weight	232.32	1527.52	1527.52	1527.48	1303.38	526.16
crystal system	Monoclinic	Monoclinic	Monoclinic	Monoclinic	Monoclinic	Monoclinic
space group	$P2_1/c$	'*P*2/n'	'*P*2/n'	'*P*2/n'	'*C*2/c'	*'C2/c'*
a (A°)	8.3343 (17)	17.4218(4)	17.4716(4)	17.4957(8)	25.6867(6)	13.5908(3)
b (A°)	8.4636(17)	9.8690(2)	9.8593(2)	9.8364(4)	9.5991(2)	11.6711(3)
c (A°)	18.908(4)	19.5378(5)	19.5176(5)	19.5011(9)	25.3877(7)	17.6727(3)
α (deg)	90.00	90.00	90.00	90.00	90.00	90.00
β (deg)	98.09(3)	90.2900(10)	90.2570(10)	90.248(3)	103.991(2)	98.023(2)
γ (deg)	90.00	90.00	90.00	90.00	90.00	90.00
V (A° 3)	1320.5(5)	3359.20(13)	3362.02(13)	3356.0(3)	6074.1(3)	2775.80(11)
Color and habit	White block	Black block	Black block	Black block	Black block	Black Rod
Z	4	2	2	2	4	4
dcal (g/cm^3)	1.169	1.510	1.509	1.512	1.425	1.259
Crystalsize (mm^3)	0.30 × 0.20 × 0.15	0.34 × 0.30 × 0.27	0.36 × 0.28 × 0.26	0.40 × 0.30 × 0.20	0.40 × 0.30 × 0.20	0.30 × 0.20 × 0.15
Temperature (K)	293(2)	293(2)	293(2)	292(2)	292(2)	292(2)
wavelength (A°)	0.71073	0.71073	0.71073	0.71073	0.71073	0.71073
μ (mm^{-1})	0.074	1.332	1.330	1.333	1.446	0.817
GOFa on F2	1.091	1.047	1.058	1.037	1.052	1.036
final R indices[I > 2σ(I)]	R1 = 0.0578 wR2= 0.1712	R1 = 0.0515 wR2= 0.1393	R1 = 0.0507 wR2= 0.1380	R1 = 0.0523 wR2 = 0.1428	R1 = 0.0444 wR2 = 0.1106	R1 = 0.0577 wR2 = 0.1617
R indices (All data)	R1 = 0.1032 wR2 = 0.2100	R1 = 0.0826 wR2 = 0.1631	R1 = 0.0819 wR2 = 0.1621	R1 = 0.0882 wR2 = 0.1681	R1 = 0.0738 wR2 = 0.1290	R1 = 0.0744 wR2 = 0.1755

Table S2 Comparative bond lengths (Å) in cubane core of **1** and **2**

Bond lengths	**1**	**2**
Cu1-O1	2.378(3)	2.328(2)
Cu2-O3	2.370(3)	2.329(2)
Cu1-O3	1.984(2)/2.005(2)	1.986(2)/2.009(2)
Cu2-O1	1.992(3)/1.997(2)	1.981(2)/2.014(2)
Cu1···Cu1	2.9825(9)	2.9977(8)
Cu2···Cu2	2.9798(9)	2.9978(8)
Cu1···Cu2	3.328/3.331	3.269/3.294

Table S3 Selected bond lengths (Å) in **H_3L1**, **1**, **2** and **3**

Bond lengths	**H_3L1**	**1**	**2**	**3**
N1-C10	1.339(3)	1.330(4)	1.321(5)	1.313(4)
N1-C2	1.449(3)	1.417(4)	1.414(4)	1.445(3)
O1-C12	1.252(3)	-	-	1.292(4)
C1-C2	1.390(3)	1.506(6)	1.522(5)	1.386(5)
C2-C3	1.396(3)	1.347(5)	1.337(5)	1.384(5)
C3-C4	1.410(3)	1.446(6)	1.475(5)	1.422(5)
C4-C5	1.399(3)	1.470(6)	1.473(6)	1.392(7)
C5-C6	1.386(3)	1.320(6)	1.320(5)	1.345(7)
C1-C6	1.393(3)	1.490(5)	1.486(5)	1.397(5)
N2-C4	1.398(3)	1.290(4)	1.282(5)	1.404(6)
C1-O1	-	1.434(4)	-	-
C12-O2	-	1.287(5)	-	-
N1-Cu2	-	1.9311(17)	1.941(3)	1.968(2)
N3-Cu1	-	1.9359(18)	1.939(3)	-
O2-Cu2	-	1.899(3)	1.896(2)	-
O4-Cu1	-	1.899(3)	1.907(3)	1.898(2)

Table S4 Selected bond angles in the cubane core of **1** and **2**

Bond angles	**1**	**2**
Cu1-O3-Cu1	96.78(10)	97.23(9)
Cu2-O1-Cu2	96.65(10)	97.26(9)
Cu1-O1-Cu2	98.83(10)/ 98.82(10)	98.37(9)/98.42(9)
Cu1-O3-Cu2	99.46(10)/ 98.73(10)	99.21(9)/97.55(9)
O1-Cu2-O1	82.11(10)	81.75(9)
O3-Cu1-O3	81.87(10)	81.78(9)
O1-Cu1-O3	80.51(10)/80.54(10)	81.11(8)/81.19(8)
O1-Cu2-O3	80.47(9)/81.00(9)	80.55(9)/81.75(8)

Table S5 UV-vis absorption bands (λ_{max}, nm, ε $M^{-1}cm^{-1}$) for **1-3** (c, 100μM, Acetonitrile)

1	**2**	**3**
430 (4.07×10^3)	410 (1.42×10^3)	
349 (4.53×10^3)	347 (8.62×10^3)	311 (7.27×10^3)
278 (9.21×10^3)	281 (8.70×10^3)	290 (8.49×10^3)

Table S6 Electrochemical (CV) data of the ligands **H_3L1**, **H_2L2**, **H_2L3** and complexes **1-3** (*c*, 100 μM, MeCN)

	Oxidation potential (V)	**Reduction potential (V)**
H_3L1	0.520	-
H_2L2	0.525	-
H_2L3	0.518	-
1	0.559	-0.896
2	0.563	-0.909
3	0.536	-0.691

Table S7 Electrochemical (DPV) data for the ligands **H_3L1**, **H_2L2**, **H_2L3** and complexes **1-3** (*c*, 100 μM, MeCN)

	Oxidation potential (V)	Reduction potential (V)
H_3L1	0.507	-
H_2L2	0.512	-
H_2L3	0.513	-
1	-	-0.875
2	-	-0.891
3	-	-0.641

References

1. D. D. Perrin, W. L. F. Armango and D. R. Perrin, *Purification of laboratory Chemicals*, Pergamon, Oxford, UK, 1986.

2. (a) G. M. Sheldrick, *SHELXL-97, Program for X-ray Crystal Structure Refinement* Gottingen University: Gottingen, Germany, 1997; (b) G. M. Sheldrick, *SHELXS-97, Program for X-ray Crystal Structure Solution* Gottingen University: Gottingen, Germany, 1997.

3. (a) A. L. Spek, *PLATON, A Multipurpose Crystallographic Tools* Utrecht University, Utrecht, The Netherlands, 2000. (b) A. L. Spek, *Acta Crystallogr. Sect. A* 1990, **46***,* C31.

4. W. J. Geary, *Coord. Chem. Rev*. 1971, **7**, 81.

5. M. Körner, P. A. Tregloan and R. van Eldik, *Dalton Trans.,* 2003, 2710.